NEAR INFRARED SPECTROSCOPY TO ASSESS THE ONSET OF INCREASED METABOLISM AND MUSCLE TISSUE OXYGENATION DURING MUSCLE CONTRACTIONS

by

Yi Sun

A dissertation submitted to the Graduate Faculty of
Auburn University
in partial fulfillment of the
requirements for the Degree of
Doctor of Philosophy

Auburn, Alabama
December 8, 2012

Key words: $\dot{V}O_2$ on-kinetics, NIRS, O_2Hb%, Mb

Approved by

L. Bruce Gladden, Chair, Professor of Kinesiology
David D. Pascoe, Professor of Kinesiology
John C. Quindry, Associate Professor of Kinesiology
Dean D. Schwartz, Associate Professor of Anatomy, Physiology & Pharmacology

Abstract

The aims of the present study were to 1) Determine whether there is a time delay (TD) in $\dot{V}O_2$ at the onset of contractions by comparing the NIRS responses during blood perfusion versus hemoglobin (Hb)-free buffer perfusion; 2) Explore the contribution of myoglobin (Mb) versus Hb to the NIRS signals during muscle contractions; and 3) Examine the correlation between venous O_2Hb% and NIRS signals under a variety of O_2 delivery and $\dot{V}O_2$ conditions. Canine gastrocnemius muscles (GS) in six dogs were isolated and pump perfused. NIRS signals were recorded continuously and venous blood was sampled intermittently at various flow rates (Control Flow, High Flow and Low Flow), and with inspired gas at three different O_2 fractions (12%, 21%, and 100%) as well as during electrically stimulated tetanic muscle contractions at the rate of 1/2 s and 2/3 s. The Mb contribution to NIRS spectra was evaluated by comparing the NIRS signals under blood perfusion to the signals during Hb-free Krebs-Henseleit bicarbonate buffer (KHBB) perfusion. The TD was determined from the fitting of deoxy- NIRS signals (HHbMb) with a monoexponential model. Venous O_2Hb% and deoxy-NIRS signals (HHbMb) were linearly correlated in the six dogs ($R^2 = 0.93 \pm 0.05$). A high linear correlation was also found between O_2Hb% and oxy-NIRS signals ($HbMbO_2$) ($R^2 = 0.92 \pm 0.03$) in five out of the six dogs. TD from the fitting of HHbMb was not significantly different between 1/2 s contractions with blood perfusion (8.4 ± 1.4 s), 2/3 s contractions with blood perfusion (6.5 ± 1.1) and 1/2 s contractions with KHBB perfusion (9.0 ± 2.7 s). The Mb contribution to NIRS signals averaged 57 ± 18% and a large inter-individual variability was observed (39 - 83%). In conclusion, the present study suggested that in the isolated, perfused canine GS model, NIRS signals well

represent venous O_2Hb% at various flow rates, with inspired gas at different O_2 fractions and during electrically stimulated muscle contractions. Surprisingly, a TD was still observed during KHBB perfusion that could be partially explained by the O_2 storage. Additionally, the Mb contribution to the overall NIRS signals is greater than 50% during muscle contractions; albeit measurement of this contribution was highly variable.

Acknowledgments

I would like to first thank Dr. Bruce Gladden, for his guidance, mentoring and caring throughout my studies during the past three and half years. To my committee members, Dr. David Pascoe, Dr. John Quindry and Dr. Dean Schwartz; thank you for serving on my committee, for your feedbacks, critiques and patience. Thank you to Dr. Doug Goodwin for contributing as my outside reader. Also thank you to Dr. James McDonald, Brian Ferguson and Matthew Rogatzki, for your assistance and input in this project. Special thanks to Dr. Mary Rudisill, Head of the Department of Kinesiology for providing me this great opportunity to study at Auburn. I would also like to thank Dr. Nicola Lai and Jessica Spires from Case Western University for providing the Macro Programs for data analysis. Lastly, I would like to thank my parents for their continuous love and support.

Table of Contents

List of Tables

List of Figures

I. REVIEW OF LITERATURE

$\dot{V}O_2$ on-kinetics

The atmosphere that we live in contains about 20.93% oxygen (O_2). O_2 is a key element that ensures the survival, locomotion, and reproduction of organisms that possess DNA-containing mitochondria, the site for O_2 consumption. The oxygen consumption ($\dot{V}O_2$) of humans is relatively low at rest, approximately 3.5 $mlO_2 \cdot kg^{-1} \cdot min^{-1}$. Any increase in activity such as walking, jogging, doing laundry, etc. will elicit an increase in energy demand and ultimately higher O_2 consumption. The study of the physiological mechanisms responsible for the dynamic $\dot{V}O_2$ response to exercise and its subsequent recovery is called $\dot{V}O_2$ kinetics (50). Similarly, the study of the physiological mechanisms for the $\dot{V}O_2$ response at the onset of exercise is referred to as $\dot{V}O_2$ on-kinetics.

At the onset of physical activity or exercise, the O_2/ATP demand is traditionally considered to increase immediately with muscle contraction; this demand is described as a "square wave" increase (43). However, the increase in oxidative phosphorylation (reflected in $\dot{V}O_2$) is not fast enough to meet ATP demand at the beginning of exercise. Instead, $\dot{V}O_2$ follows an exponential pattern of increase (e.g., Figure 1) (38, 103). The discrepancy between O_2 demand and O_2 supply is called "oxygen deficit" (60).

The stored ATP level is low, about 3 $mmol \cdot kg^{-1}$ in most tissues and 6 $mmol \cdot kg^{-1}$ in skeletal muscle (46). Therefore, the high demand for ATP during exercise is mainly met by replenishment. ATP utilization (and therefore demand) can increase by as much as 100-fold for skeletal muscle during the transition from rest to contractions (91). ATP is produced via three

pathways: immediate, glycolytic and oxidative. In the immediate pathway (reaction 1), phosphocreatine (PCr) reacts with ADP to produce ATP. The stored PCr concentration ([PCr]) in skeletal muscle is several times higher than that of ATP, in the range of 18-20 $mmol \cdot kg^{-1}$ wet muscle (or 23-26 mM) (46). But that's still only sufficient for a short period of contractions/exercise (44). The PCr is used as an immediate source for ATP replenishment. In the second pathway, glucose/glycogen is the main fuel source via glycolysis/glycogenolysis (reactions 2 & 3). Glucose or glycogen can be converted to pyruvate or lactate, with no requirement for consumption of O_2 (24). One glucose molecule can be used to produce two ATP molecules and two reduced nicotinamide adenine dinucleotide (NADH) electron carriers. Finally, the oxidative pathway (O_2-requiring) is known as oxidative phosphorylation. It occurs in mitochondria, where O_2 molecules are reduced and ATP is produced via the electron transport chain in the inner membrane (reaction 4) (101).

Phosphocreatine reaction:
$PCr + ADP \leftrightarrow Cr + ATP$ ..... reaction 1

Glycolysis from glucose:
$Glucose + 2ADP + 2Pi + 2NAD^+ \rightarrow 2lactate + 2ATP + 2NADH + 2H^+$ ..... reaction 2

Glycolysis from glycogen:
$Glycogen_n + 3ADP + 3Pi + 2NAD^+ \rightarrow$

$glycogen_{n-1} + 2lactate + 3ATP + 2NADH + 2H^+$ ..... reaction 3

Oxidative phosphorylation:
$NADH + H^+ + 3ADP + 3P_i + \frac{1}{2}O_2 \rightarrow 3ATP + NAD^+ + H_2O$ ..... reaction 4
(The actual P:O ratio is approximately 2.5; 3 is used in this equation for convenience.)

Figure 1. Taken from Whipp et al. (103). Graphical depiction of $\dot{V}O_2$ during exercise. The increase in O_2 demand is considered to follow a "square wave" pattern. The difference between O_2 demand and O_2 consumption at exercise onset is called "O_2 deficit".

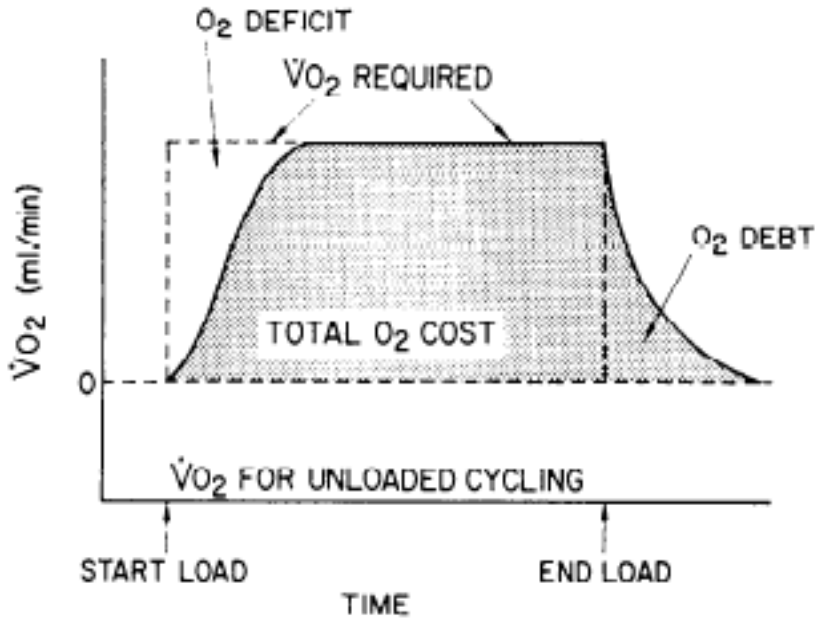

Estimates have been made of the time required for each of the three pathways to reach peak power: immediate system, ≈1 s; glycolytic system, ≈7 s; oxidative system, ≈180 s (81). Numerous studies (7, 19, 26, 62, 90) have attempted to address the factors that regulate or control oxidative phosphorylation. Two classical hypotheses have been suggested to explain its relative slowness in comparison to the other two energy systems; these are 1) O_2 delivery and 2) requirement for activation of cellular reactions. These two hypotheses will be discussed in detail below.

In humans, measurement of the $\dot{V}O_2$ response to exercise is mainly based on breath-by-breath gas analysis at the mouth. The measured $\dot{V}O_2$ is called pulmonary $\dot{V}O_2$ ($\dot{V}O_2p$). The $\dot{V}O_2p$ response at the onset of exercise is composed of three phases (Figure 2). Phase 1 is also called the "cardiodynamic phase". The venous blood draining the contracting muscle that contains lower O_2 content will not affect pulmonary gas exchange during the transit delay to the lungs at

the onset of exercise. Therefore, it is not likely that the mixed venous O_2 tension has changed and caused an increase in $\dot{V}O_2$ within the first breath of exercise. During this phase, ventilatory and gas-exchange responses are proportional to an increased pulmonary blood flow. A high correlation has been shown to exist between the magnitude of gas exchange response and response of heart rate (104). The $\dot{V}O_2$p and muscular $\dot{V}O_2$ ($\dot{V}O_2$m) are dissociated from each other in this phase (88). Phase 1 is not normally taken into account in the modeling of $\dot{V}O_2$ on-kinetics. $\dot{V}O_2$ in Phase 2 is well-characterized by a mono-exponential function with a time delay. $\dot{V}O_2$p is considered to reflect $\dot{V}O_2$m in this phase (87). Phase 3 is either a steady state, or a slow component phase of $\dot{V}O_2$ response depending on the exercise intensity. The slow component is usually seen in exercise at intensities above the lactate threshold (LT). It was traditionally considered to be due to progressive recruitment of less efficient type II muscle fibers (20). However, this theory was challenged by Zoladz et al. (112) when reanalyzing the data from a previous study with the canine model. With tetanic contractions corresponding to 60-70% of $\dot{V}O_{2peak}$, even though absolute changes in $\dot{V}O_2$were not seen, a "slow component-like response" was observed when $\dot{V}O_2$ was normalized to peak force. Peak force declined while $\dot{V}O_2$ remained constant, thus the $\dot{V}O_2$/force ratio increased. Since all of the muscle fibers were synchronously activated by electrical stimulation in this study, recruitment of more muscle fibers would not be the explanation for the slow component. While the debate about underlying causes of the $\dot{V}O_2$ slow component continues, this study (112) indicates that metabolic factors might play a role, independently of fiber type.

Figure 2 illustrates the three phases of the $\dot{V}O_2$ response to exercise.

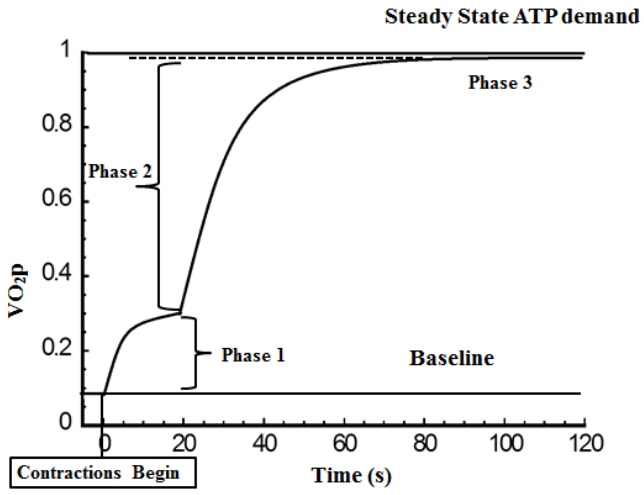

The mono-exponential increase of $\dot{V}O_2$ in Phase 2 has been described by the following equation and is illustrated in figure 3:

$$y(t) = y_{bas} + A\,[1 - e^{-(t-TD)/tau}]$$

where y_{bas} is the baseline value at rest before contractions onset; A is the amplitude between y_{bas} and the asymptote of the primary component (Phase 2); t is time; TD is the time delay, which is the time obtained from the fitting procedure and corresponds to the delay before the response becomes mono-exponential; and tau is a time constant, which is ≈63% of the time required for $\dot{V}O_2$ to rise from y_{bas} to the asymptote of the mono-exponential function. The sum of tau and TD is referred to as the mean response time (MRT).

Figure 3 describes the mono-exponential curve and components of Phase 2 of the $\dot{V}O_2$ response to exercise.

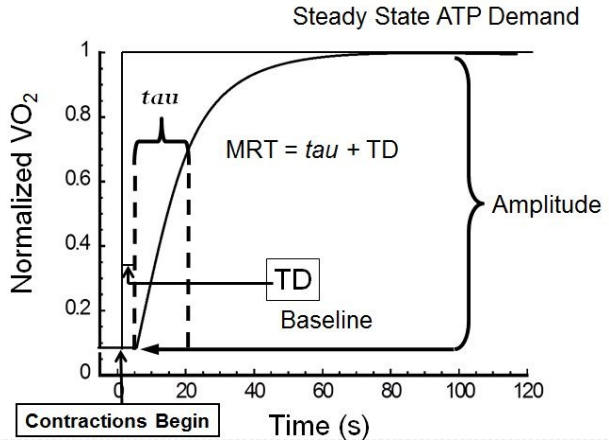

Hypothesis 1: O_2 delivery

As stated above, broadly speaking, two hypotheses have been suggested to explain the slow turn-on of oxidative phosphorylation at exercise onset, and one of them is limitation in O_2 delivery. In humans, the kinetics of blood flow (Q, tau = 6.4-12.8 s) is about twice as fast as that of $\dot{V}O_2$ (tau = 16.6-18.8 s) with exercise intensity under LT (62). Also, during supra-LT knee extension exercise in humans, the tau of femoral Q is faster than that of $\dot{V}O_2$ (19). In the same study (19), $\dot{V}O_2$ kinetics was faster with priming contractions while the kinetics of Q was unchanged. Furthermore, muscle deoxygenation during transition from unloaded cycling to constant-load cycling either below or above ventilatory threshold (VT) was unchanged (8.9 s below VT vs. 6.4 s above VT) (35). All of these results are evidence against the O_2 delivery hypothesis. In other words, O_2 delivery does not appear to be a limiting factor for slow $\dot{V}O_2$ kinetics at exercise onset (36) for submaximal (below LT) intensity under normal conditions.

On the other hand, Goodwin et al. (26) found that slowed O_2 delivery (below the normal spontaneous level), achieved by slowing blood flow kinetics, resulted in a linear slowing of $\dot{V}O_2$

kinetics at exercise onset in the isolated, perfused canine gastrocnemius complex (GS) *in situ*. In Goodwin's study (26), the blood flow on-kinetics was set at three levels: a control trial with MRT of 20 s and two experimental trials with MRT of 45 s and 70 s, respectively. Hypoxia also has an effect on $\dot{V}O_2$ on-kinetics. In humans, decreased O_2 delivery via breathing 14% O_2 slowed $\dot{V}O_2$ on-kinetics, while hyperoxia (70% O_2) did not speed the on-kinetics (48). Putting all the evidence together, it appears that the normoxic spontaneous blood flow condition provides just the right amount of O_2 delivery for $\dot{V}O_2$ on-kinetics in submaximal exercise or contractions. Therefore, providing additional O_2 has no effect, whereas reducing O_2 availability slows the $\dot{V}O_2$ on-kinetics (26).

Hypothesis 2: metabolic activation

For control of $\dot{V}O_2$ on-kinetics, the alternative to O_2 delivery is metabolic activation. However, to be clear, O_2 delivery and metabolic activation are not mutually exclusive (101). Several factors may play a role in this hypothesis, such as [ADP], pyruvate dehydrogenase (PDH) activity, inhibition of mitochondrial oxidative phosphorylation by nitric oxide (NO), etc. PDH is considered to be the rate limiting enzyme for entry of carbohydrates (CHO) into the tricarboxylic acid (TCA) cycle, and therefore a potentially limiting site for $\dot{V}O_2$ on-kinetics at exercise onset. For humans, when exercising in hypoxia (breathing 11% O_2) for 1 min at 50-55% $\dot{V}O_2$max, lactate accumulates (53) perhaps partly due to low PDH activity (78). Dichloroacetate (DCA) has been shown to activate PDH at rest and to maintain an enhanced activation level during the first minute of cycling at submaximal intensity in humans; this resulted in increased [acetyl-CoA] and decreased [lactate] (79). PCr breakdown and glycogenolysis were shown to be lower with DCA in the same study (79). Reduced PCr breakdown and lower blood [lactate] were also observed by Rossiter et al. (90) during high-intensity knee extensions in humans, which corresponded to 70%

of $\dot{V}O_2$. However, the tau values for PCr breakdown and $\dot{V}O_2$ kinetics were not different between the control group and DCA group. In another study (7) with one-legged knee-extensor exercise at supramaximal intensity in humans (110% of thigh peak $\dot{V}O_2$); thigh $\dot{V}O_2$, PCr utilization and lactate production were the same between a control group and a DCA group, despite higher PDH activity in the latter group during the first 15 s of exercise. PCr utilization and lactate production were also not affected by DCA infusion during 10 s all-out cycling (47) with human subjects. Therefore, there is no clear experimental evidence so far supporting that PDH is a rate limiting enzyme that causes slow $\dot{V}O_2$ on-kinetics.

At the onset of exercise, [ADP] increases, moving toward its Km (89). The increase in [ADP], together with increased [Pi] is one of the driving forces for the electron transport chain and oxidative phosphorylation. Inhibition of PCr breakdown has been shown to cause increased [ADP] (55). Less PCr was depleted and higher [ADP] was observed in creatine kinase (CK, which catalyzes the breakdown of PCr) knockout mice during electrically stimulated twitch contractions (86), when assessed with ^{31}P-magnetic resonance spectroscopy (MRS). In this study, PCr hydrolysis could only explain about 1/3 of ATP utilization within the first 2 s of contractions in CK knockout mice. Among other sources of ATP (net ATP depletion, glycolysis and oxidative phosphorylation), inclusion of oxidative phosphorylation in the kinetic model best reproduced PCr depletion in both wild type mice and CK knockout mice at contractions onset. This led to the conclusion that inhibition of CK accelerated activation of oxidative phosphorylation at exercise onset. However, it is noteworthy that the increased mitochondrial content in these CK knockout mice could have played a role in the faster activation of oxidative phosphorylation.

In the final steps of oxidative phosphorylation, electrons are passed down the electron transport chain (ETC) and are eventually accepted by O_2 molecules. Nitric oxide (NO) is known

to have a high affinity for the O_2-binding site, cytochrome c oxidase. Physiological levels of NO can inhibit cytochrome c oxidase, and therefore, oxidative phosphorylation (97). Therefore, it was hypothesized that inhibition of NO synthase (NOS) by $_L$-NAME could possibly expedite turn-on of $\dot{V}O_2$ kinetics at exercise onset. This hypothesis was confirmed in horses during moderate intensity ($7 m \cdot s^{-1}$) (58) as well as during high intensity treadmill running (80% of peak $\dot{V}O_2$) (57), for both of which there was a significantly reduced tau. Similar findings were seen in humans during moderate intensity (90% of gas exchange threshold) (51) and heavy intensity cycling (40% of the difference between the gas exchange threshold and peak $\dot{V}O_2$) (52). In these studies (14, 51, 52), the tau for $\dot{V}O_2$ was decreased with the addition of $_L$-NAME. However, it is known that NO also has a vasodilatory effect. Inhibition of NOS could cause vasoconstriction as a result. In order to eliminate the vasoconstriction effect of $_L$-NAME, blood flow was maintained constant in a study by Grassi et al (32) employing the isolated, perfused canine GS model. It turned out that inhibition of NOS activity by $_L$-NAME did not accelerate $\dot{V}O_2$ on-kinetics in this preparation. Even though less fatigue was seen in contractions corresponding to 60% of $\dot{V}O_2$peak with the addition of $_L$-NAME, neither tau nor TD of $\dot{V}O_2$ was significantly different from the control group. It seems that at least in this model, inhibition of cytochrome c oxidase activity by NO does not change the speed of $\dot{V}O_2$ kinetics at exercise onset.

Other studies in isolated, perfused canine skeletal muscle

The limiting factors of $\dot{V}O_2$ on-kinetics have been investigated in a series of studies in the Gladden laboratory over the past few years. An isolated canine GS model has been used. Briefly, the animals are anesthetized and the GS is surgically isolated, so that the blood flow to and from the muscle is only through the popliteal artery and popliteal vein, respectively. This allows for

blood flow control with a pump and infusion of pharmacological agents directly into the muscle (63). The sciatic nerve is exposed for electrically-elicited tetanic contractions.

The role of convective O_2 delivery ($Q \times CaO_2$) was investigated first (28). In this study, a control condition was defined as electrically stimulated tetanic contractions with spontaneous adjustment of blood flow at 60-70% $\dot{V}O_2$peak. The control condition was compared to the pump-perfused condition, in which blood flow was set prior to contractions at the level that was previously reached during the steady state of contractions in the control condition. As a result, the tau of $\dot{V}O_2$ in the control condition was not different from that of the pump-perfused condition. This observation argued that at least at this submaximal intensity of muscle contractions, convective O_2 delivery is not the limiting factor for $\dot{V}O_2$ on-kinetics. To examine if this statement is also true at higher exercise intensities, another study was carried out by the same group (31). The experimental design was the same as the earlier study, except that the GS muscle was stimulated to contract at an intensity corresponding to $\dot{V}O_2$peak. Unlike the previous study, the $\dot{V}O_2$ tau was significantly faster in the pump-perfused condition (18.5 s) than the control condition (24.9 s). Therefore, for isolated canine muscle model, O_2 delivery is a limiting factor for $\dot{V}O_2$ on-kinetics at a stimulation rate that elicits $\dot{V}O_{2peak}$, but not at lower, submaximal metabolic rates. However, it was not clear whether a slower than normal convective O_2 delivery would slow $\dot{V}O_2$ on-kinetics during muscle contractions at a submaximal metabolic rate. Therefore, another study was conducted to investigate this issue, and as mentioned earlier, results from the study of Goodwin et al. (26) suggested that slowed O_2 delivery caused a linear slowing of $\dot{V}O_2$ on-kinetics.

Even though bulk O_2 delivery may not play a key role in $\dot{V}O_2$ on-kinetics, the lag in $\dot{V}O_2$ increase at exercise onset might be due to a delay in O_2 diffusion from capillaries to tissues. According to Fick's law of diffusion, $\dot{V}O_2 = DO_2 \times (P_{cap}O_2 - P_{mito}O_2)$. DO_2 is the diffusing capacity (conductance factor) that incorporates all the steps in the O_2 diffusing pathways from Hb to mitochondria (45). $P_{cap}O_2$ and $P_{mito}O_2$ represent mean capillary PO_2 and mitochondrial PO_2, respectively. In order to answer the question about O_2 diffusion, three conditions were compared by Grassi and colleagues with the canine model (29). For all three conditions, blood flow was elevated prior to contractions to the level that was achieved at the steady state of a preliminary bout of contractions. Normoxic gas was breathed for the control condition and hyperoxic gas (100% O_2) for the second and third conditions. In the third condition, RSR-13 was also infused into the animal. RSR-13 is an allosteric modifier of Hb and has been shown to induce a rightward shift of the oxyhemoglobin dissociation curve and cause an increase in $\dot{V}O_2$max (85). $P_{cap}O_2$ was estimated to be highest in hyperoxia + RSR-13 (197 Torr), medium in hyperoxia only (97 Torr), and lowest in normoxia (53 Torr). Regardless of significant differences in $P_{cap}O_2$; however, $\dot{V}O_2$ tau was similar across the three conditions. Therefore, O_2 diffusion did not appear to be a limitation for $\dot{V}O_2$ on-kinetics at submaximal metabolic rates. When all of these GS studies on O_2 delivery and diffusion are considered, it appears that the muscle typically operates spontaneously at just the required level of O_2 availability at submaximal metabolic rates such that speeding or increasing O_2 supply has no effect on $\dot{V}O_2$ on-kinetics whereas a slowing or reduction of O_2 supply slows the $\dot{V}O_2$ on-kinetics. In other words, spontaneously perfused skeletal muscles appear to operate near the so-called tipping point of O_2 delivery (26, 80).

It was known that $\dot{V}O_2$ on-kinetics of a bout of contractions is speeded by a priming bout of contractions in humans (14). This finding was also examined in the canine model (41). The GS muscle was stimulated to contract for 2 min at ~70% $\dot{V}O_2$peak. The second bout of contractions was elicited again after a 2-min recovery. It was found that the tau of Phase 1, and the amplitude of the slow component were decreased in the second bout compared to the first one. Besides $\dot{V}O_2$ on-kinetics, blood flow on-kinetics was speeded too, and O_2 extraction was also greater in the second bout. Faster O_2 delivery (faster blood flow kinetics) in the second bout could be the reason for faster $\dot{V}O_2$ on-kinetics. However, it is also likely that metabolic activation was greater at the onset of bout 2 although metabolites such as ADP and PCr were not measured in this study.

The other hypothesis for slow O_2 on-kinetics is what some investigators have called "metabolic inertia." A series of factors in this hypothesis has been studied with the canine model. As mentioned above, PDH is the rate limiting enzyme for entry of carbohydrate into the TCA cycle. And in humans, DCA, as the PDH inhibitor did not cause differences in PCr utilization and lactate production during supramaximal exercise (7). A similar result was observed with the canine model (30). Even though DCA activated PDH at rest (as evidenced by markedly elevated acetylcarnitine concentration), PCr degradation and lactate production were not different from the control group following muscle contractions at 60-70% of $\dot{V}O_2$peak. Of greater importance for the present discussion, the tau of $\dot{V}O_2$ was not different between the DCA group (24.5 s) and control group (22.3 s). As stated above, the effect of $_L$-NAME was investigated in the dog model also (32), and no differences in $\dot{V}O_2$ on-kinetics were found between the $_L$-NAME treated group and the control group. Another factor that was examined using the canine model was CK activity. In a study by Grassi et al. (37), iodoacetamide (IA) was used to inhibit CK. Significant fatigue

(fatigue index 0.67 on a scale of 1) was seen during tetanic contractions at 70% of $\dot{V}O_2$peak with IA while no fatigue was observed in the control group. With regard to $\dot{V}O_2$ analysis, besides the traditional fitting model that is usually used in $\dot{V}O_2$ on-kinetics studies, a second model was used in this study to account for the time-dependent alterations in the 'error signal' in the IA group. With either model, the $\dot{V}O_2$ on-kinetics in the IA group was faster than that of the control group, as suggested by a smaller tau in the IA group. It seems that the buffering of ATP by PCr at exercise onset slows the activation of oxidative phosphorylation, and therefore, slows $\dot{V}O_2$ on-kinetics.

TD in $\dot{V}O_2$ on-kinetics

As noted above for work with the GS model, fitting of the $\dot{V}O_2$ on-kinetics response always includes a TD before the response becomes fully mono-exponential (or mono-exponential plus a slow component). This has led to a further question as to whether or not there is any "true" delay in the increase of $\dot{V}O_2$ at contractions onset. There have been some controversial results regarding this question. A small TD (4.9 s – 6.1 s) has been found in canine studies on the basis of the exponential model described earlier (30, 31, 41). However, inspection of the actual $\dot{V}O_2$ values also shows that there is some increase in $\dot{V}O_2$ during the period of the TD (107). Using the phosphorescence quenching technique to measure extracellular PO_2 at the single muscle fiber level, and thereby muscle fiber $\dot{V}O_2$, a TD (2.1 s) was also found in the lumbrical muscles of *Xenopus laevis* with repetitive tetanic contractions (0.33 Hz) (56). To the contrary, in another study with 1 Hz twitch contractions in rat spinotrapezius muscle, no TD was found in $\dot{V}O_2$m, which was calculated based on capillary red blood cell flux and microvascular PO_2 (9). A similar finding was reported by Takakura et al. (98). No TD was observed in $\dot{V}O_2$

when the rat hindlimb was stimulated to contract with twitches at 1 Hz to obtain 50%, 75% and 100% of peak twitch tension with pump-perfusion of Hb-free artificial buffer. In humans, the $\dot{V}O_2$ at the onset of 1-s duration maximal isometric ankle dorsiflexion contraction at 60 to 80-s intervals did not show a major TD either (99); this was determined on the basis of modeling from PCr recovery rate following contractions. Therefore, there is no consensus as to whether there is a time delay in the increase in $\dot{V}O_2$ during the transition from one metabolic rate to another. The different findings could be due to the different techniques that were utilized. For example, with the isolated canine muscle model, the reported time delay is possibly due to the transit time from muscle fibers where metabolism actually happens, to the measurement site of $\dot{V}O_2$ in the vein exiting the muscle. In the present study, we will attempt to investigate the issue of time delay with near-infrared spectroscopy (NIRS). More details about NIRS will be discussed below. Briefly, the relative oxygenation status of both hemoglobin (Hb) and myoglobin (Mb) together is "seen" by NIRS. However, with Hb-containing blood flowing through the muscle, O_2 utilization can be matched by O_2 delivery either entirely or partially, thus creating a time delay in any change in the NIRS signal. We hope to circumvent this issue by replacing blood with Krebs-Henseleit bicarbonate buffer, so as to eliminate the Hb signal.

$\dot{V}O_2$ on-kinetics and diseases

Exercise testing is commonly incorporated in clinical treatment, providing functional, diagnostic, and prognostic assessments for cardiopulmonary patients (3). $\dot{V}O_2max/\dot{V}O_2peak$ from exercise testing is considered the gold standard for prognosis for heart failure (2). A lower maximal or peak $\dot{V}O_2$ is usually seen in patients with chronic diseases, such as heart failure (2), COPD (84), and peripheral arterial disease (PAD) (42).

Besides low $\dot{V}O_2$peak/$\dot{V}O_2$max, patients with diseases that limit blood flow, O_2 extraction, O_2 saturation or the combination of the three are found to have slower $\dot{V}O_2$ on-kinetics. For example, an increase in pulmonary blood flow, reflected by $\dot{V}O_2$ increase during the first 20 seconds of exercise was diminished in patients with congenital heart disease during submaximal exercise (95), and the Phase 2 of $\dot{V}O_2$ kinetics was also slower for this group of patients. For mildly hypoxemic COPD patients, hyperoxic (30% O_2) air breathing resulted in a faster tau for the Phase 2 $\dot{V}O_2$ response (77). Besides limitation in O_2 supply, the fact that invasive revascularization for PAD patients did not completely normalize exercise performance (13) led to the investigation of other factors such as metabolic myopathy, either genetically determined or acquired. Grassi et al. demonstrated that patients with metabolic myopathies such as mitochondrial myopathies (MM) and McArdle's diseases (McA) had a higher than normal O_2 delivery and slower $\dot{V}O_2$ on-kinetics (34). When an additional study was done to further examine this issue with near-infrared spectroscopy (NIRS), patients with MM or McA had impaired O_2 extraction and that the peak of O_2 extraction was found to be linearly correlated with $\dot{V}O_2$peak (33). Other population groups such as diabetic patients and aging people have also been reported to have slowed $\dot{V}O_2$ on-kinetics. The observation that diabetic patients had slower $\dot{V}O_2$ kinetics compared to overweight nondiabetics and lean nondiabetics (12) suggested that it was specifically diabetes, not obesity that affected $\dot{V}O_2$ responses. A study on men aged 30-80 yrs revealed an average increase of 0.67 $s \cdot yr^{-1}$ for tau (5).

Hemoglobin (Hb), myoglobin (Mb) and NIRS

In vertebrates, Hb is an $\alpha_2\beta_2$ tetrameric hemeprotein contained in the cytosol of erythrocytes (15). The majority of O_2 in the blood is bound to Hb (82). Hb is responsible for

binding to O_2 at the lungs and transporting the bound O_2 throughout the body to cells where O_2 is used in the aerobic pathways. Therefore, Hb is also referred to as "O_2 transport protein". Mb is an oxygen-binding cytoplasmic hemeprotein which consists of a single polypeptide chain of 154 amino acids (74). It is found in skeletal muscle fibers and cardiac muscle. Mb reversibly binds to oxygen and facilitates oxygen transport from cell membrane to mitochondria.

One Hb molecule can bind up to four O_2 molecules, while each Mb can only bind to at most one O_2 molecule. The binding of O_2 to Hb exhibits positive cooperativity, which means that binding the first O_2 facilitates subsequent O_2 binding to other subunits (15). Therefore, the dissociation curve of Hb follows a sigmoidal pattern, while that of Mb follows a hyperbolic function. Hemoglobin is about 97% saturated with O_2 when the PO_2 is 100 mmHg, and is around 75% saturated at a PO_2 of 40 mmHg. Myoglobin, on the contrary, has a much higher affinity for O_2. NMR measurements have shown that myoglobin is over 90% saturated at rest in humans (16, 83). The P_{50} of Mb (the PO_2 at which O_2 is bound to 50% of the Mb molecules) is reported to be 2.39 mmHg at 37°C and pH of 7.0 with multiwavelength optical spectroscopy (93). The P_{50} value is much higher for Hb, about 26 mmHg.

NIRS has been used to noninvasively estimate muscle oxygenation at the microvascular level for years. It was first used to investigate and monitor cerebral oxygenation (23). Later on, its application was extended to the study of muscle oxidative metabolism (92, 110), neonatal intensive care (1), anesthesia (65), activation of cerebral cortex (71), cerebral blood flow (73) and cerebral blood volume (109). The physical principle of NIRS is based on the absorption and scattering of light (75). In the window of near infrared region where the wavelength of light is between 650 and 900 nm, photons can penetrate to deeper structures, such as muscle tissues and cerebral cortex for measurement of tissue oxygenation. The light passes into arteries, arterioles,

capillaries, venules and veins. Light emitted into large vessels, such as arteries and veins is almost completely absorbed because of the large quantity of Hb. Conversely, the extent of absorbance of light passing through small capillaries is determined by the molar concentrations of chromophores, specifically Hb in the capillaries and Mb in the tissue itself. Therefore, changes in Hb and Mb concentrations can be determined by differential light absorbance (10). As illustrated in Figure 4, near-infrared (NIR) light is emitted from an optode at one or more wavelengths. The NIR light is detected by another optode and the signal is transmitted to a data acquisition device. Because of the random scattering of light by tissue, the photons can take an infinite number of paths between the light source and detector with different probabilities of survival (54). For ease of calculation and comparison, researchers have proposed a concept called “mean photon path” based on the Monte Carlo simulation method (76), which features a banana-shaped route (54).

The NIRS technique relies on the Lambert-Beer Law, which was reported by August Beer in 1851. According to this law,

$$OD_\lambda = \varepsilon_\lambda \cdot C \cdot L$$

In this equation, λ is the wavelength (nm) used; ε_λ is the extinction coefficient of the chromophore that absorbs the light ($mM^{-1} \cdot cm^{-1}$); C is the concentration (mM) of the chromophore; and L is the distance (cm) between light entry and light exit point. However, the Lambert-Beer law specifically applies to a clear, non-scattering medium. Because animal tissue is considered to be a scattering medium, and the mean photon path follows a banana-shaped route, instead of the shortest path between the light entry and light exit point, an additional correction factor called “differential pathlength factor (DPF)” (102) is added to the above equation. Therefore, the modified Lambert-Beer law for NIRS is (4):

$$\Delta OD_{\lambda} = \varepsilon_{\lambda} \cdot \Delta C \cdot L \cdot DPF$$

In this modified equation, λ is the wavelength (nm) used and ΔC is the change in concentration (mM) of the chromophore.

Figure 4: Schematic depiction of the path of light (random scattering of photons) inside the tissue. Redrawn from (4).

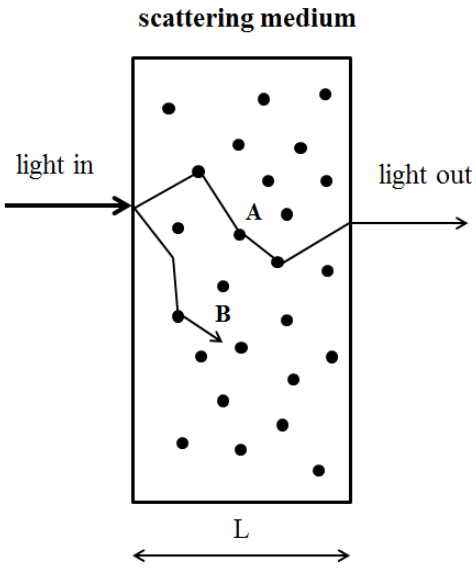

Besides scattering, another factor that affects the overall light absorbance is the molecular properties of chromophores within the light path. For example, the oxygenation status in some compounds, such as Hb and Mb can affect absorption of light. The reason lies in the different extinction coefficients of oxy- versus deoxy- groups. Figure 5 illustrates the differential extinction coefficient by oxy-[Hb + Mb] ($HbMbO_2$) and deoxy-[Hb + Mb] (HHbMb). Similarly, for the two wavelengths chosen (Figure 6), $HbMbO_2$ has a higher absorbancy at 850 nm, while HHbMb has a higher absorbancy at 760 nm. According to the Lambert-Beer law,

$$\Delta OD_{\lambda 1} = \varepsilon_{HHbMb\lambda 1} \cdot \Delta C_{HHbMb} \cdot L \cdot DPF_{\lambda 1} + \varepsilon_{HbMbO2\lambda 1} \cdot \Delta C_{HbMbO2} \cdot L \cdot DPF_{\lambda 1}$$

$$\Delta OD_{\lambda 2} = \varepsilon_{HHbMb\lambda 2} \cdot \Delta C_{HHbMb} \cdot L \cdot DPF_{\lambda 2} + \varepsilon_{HbMbO2\lambda 2} \cdot \Delta C_{HbMbO2} \cdot L \cdot DPF_{\lambda 2}$$

In the above two equations, λ1 and λ2 are the two wavelengths chosen for analysis. The difference in light absorbance at the two wavelengths is more sensitive to heme oxygenation, while the sum of the signals indicates total heme content (69).

Figures 5 and 6: Figure 5 (left) is from Moyle (72) and describes the extinction coefficient of HbO_2 and Hb at various wavelengths. Figure 6 (right) is from McCully & Hamaoka (69) and depicts the absorbancy of light by HbO_2 and Hb at various wavelengths.

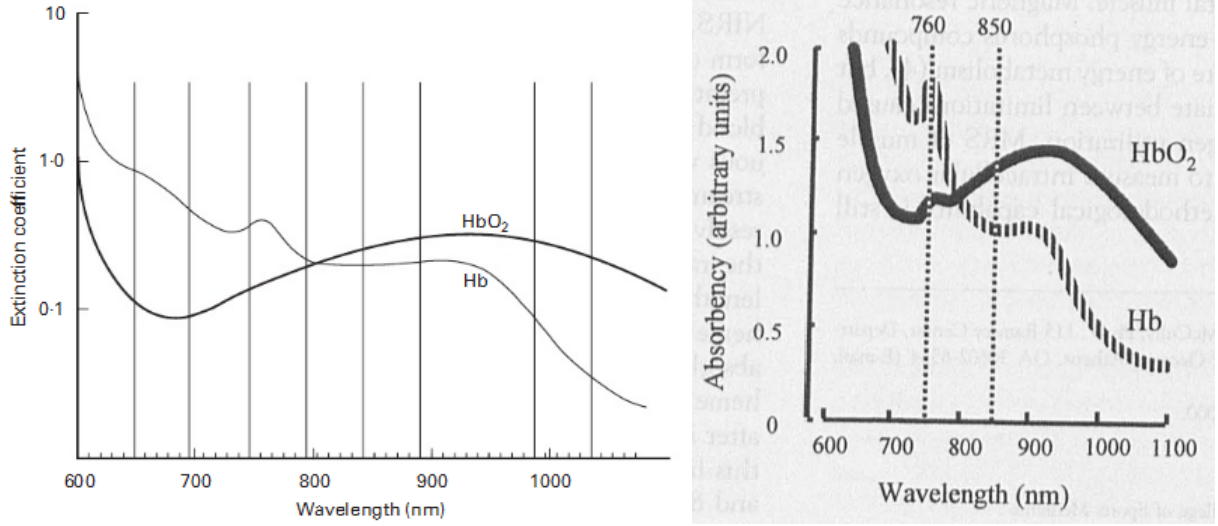

The pattern of changes in the NIRS signal during exercise has been investigated in several studies. During the transition from 20W to a work rate corresponding to 80% of LT in human cycling exercise; HHbMb increased with a TD of 13 s and tau of 10 s (18). The changes in $HbMbO_2$ and HHbMb reflect the extent of O_2 extraction, or the balance between O_2 supply and O_2 consumption. The change in HHbMb follows an exponential function (after a time delay at exercise onset) during constant work rate exercise (18), and a sigmoid function during incremental ramp exercise (22). When NIRS changes were examined during electrically stimulated muscle contractions in isolated, perfused canine GS model, the results were similar to those found in humans with constant work rate exercise; there was a time delay followed by a

monoexponential response with TD and tau values that were broadly similar to those for the $\dot{V}O_2$ response (41).

Limitations of NIRS

Even though NIRS is a convenient tool to noninvasively monitor tissue oxygenation status, it still has many limitations (21).

a. Placement of the optode: a stable contact between the optode and tissue surface is crucial to the accuracy of measurements. Dark hair tends to attenuate light.
b. Depth of tissue: Even though near-infrared light has a deeper penetration into tissues compared to visible light, typical depth sensitivity of most NIRS devices is about 1.5 cm (21), but can be as high as 2-6 cm (10). Other surface tissue such as skin and subcutaneous fat will blunt the signal.
c. The influence of blood flow/volume: A change in blood flow and blood volume is known to affect the NIRS signal. However, there is evidence that the HHbMb signal is less affected by variations in flow and blood volume (18, 35).

Besides the issues mentioned above, there are two additional limitations on the use of NIRS to quantify Hb and Mb. First, the amount of light scattered away from the straight line path is unknown. The scattering pattern of tissue can only be estimated. Secondly, it is at heme groups where absorption of light is altered by oxygenation (69), and since heme groups exist in both Hb and Mb, the absorption spectra cannot be distinguished between HbO_2 and MbO_2, or between HHb and HMb. In some studies, the contribution of Mb to the NIRS signal was reported to be less than 10% in rats (94), minimal in humans (66) and zero in isolated canine gracilis muscle (105). In other studies, Mb was estimated to contribute 50% (67) and the majority (100) of the NIRS signal. In another study (64), the relative contribution of Hb and Mb to the NIRS signal

was investigated via simulation with a mathematical model based on experimental results in humans. Under both normoxia and hypoxia (12% O_2), Mb contribution to the NIRS signal was approximately 30-35%. In summary, there is no definite conclusion regarding the extent to which Hb and Mb contribute to the NIRS signal, due to the different indirect approaches used. Besides Hb and Mb, cytochrome oxidase is another substance that has heme groups. However, the contribution of cytochrome oxidase to the NIRS signal is considered to be negligible at only about 2-5% (10).

In order to eliminate the effect of Hb on the NIRS signal, buffer was used to replace blood perfusion in a rat model (98). With stimulated twitch contractions, Mb saturation decreased linearly with increasing contraction intensity. Both the rate of increase in muscle $\dot{V}O_2$ and the rate of Mb desaturation increased with higher contraction intensity. However, a significant concern with this study (98) is that twitch contractions instead of tetanic contractions were used and a staircase pattern was seen in muscle force and $\dot{V}O_2$. Perhaps more importantly, even the highest $\dot{V}O_2$ measured (0.69 $\mu mol \cdot g^{-1} \cdot min^{-1}$) was less than twice as high as the resting value (0.46 $\mu mol \cdot g^{-1} \cdot min^{-1}$). Further study using tetanic contractions (to elicit much higher metabolic rates) with buffer perfusion would provide more information regarding the kinetics of Mb desaturation at the onset of exercise.

NIRS and venous Hb O_2 saturation (venous O_2Hb%)

NIRS has been used extensively to monitor tissue oxygenation status. The rationale for this can be ascertained from application of the Fick principle to tissue (muscle) metabolic rate as follows:

$$\dot{V}O_2 = Q \bullet CaO_2 - Q \bullet CvO_2$$

$$\therefore CvO_2 = CaO_2 - \dot{V}O_2/Q$$

and we assume that venous $O_2Hb\% \cong CvO_2$, where venous $O_2Hb\%$ is the percent saturation of Hb with O_2 in the venous blood. The question then is to what extent changes in tissue HHbMb or $HbMbO_2$ reflect changes in venous $O_2Hb\%$ ($\cong CvO_2$) under various conditions (39). A cerebral oximeter is a device that is commonly used in clinical settings to monitor brain oxygenation, especially during surgery under anaesthesia, and for stroke patients (21). Kim and colleagues (54) reported that $O_2Hb\%$ measured in jugular venous blood (jugular venous $O_2Hb\%$) was linearly correlated with HbO_2 saturation measured with cerebral oximetry (NIRS-HbO_2 normalized by Hb_{tot}) with an average correlation coefficient of 0.9 ± 0.09 during both hypercapnic/hypoxic and normocapnic/hypoxic conditions in humans. The correlation of venous $O_2Hb\%$ and NIRS signal was also investigated during exercise in deep arm muscles in humans (66). In this study, a blood pressure cuff was placed around the upper arm. When the blood pressure cuff was inflated to over 200 mmHg, the NIRS HHb spectra (the differential absorption of 760 nm and 800 nm of light) observed was considered to represent maximal Hb deoxygenation. The NIRS signal following release of the cuff was considered to reflect maximal Hb oxygenation. The maximal range of NIRS changes was used to standardize changes in deoxygenation during contractions. The NIRS data and blood samples from a forearm vein were continuously collected while subjects depressed a lever that lifted a weight every 4 s for the duration of 2 min at the work rate of 0.1 to 0.6 W. The R value for the correlation between the NIRS signal and venous Hb saturation averaged 0.92 ± 0.02.

Other evidence suggests that the oxy- signal of NIRS (NIRS-HbO_2) and venous $O_2Hb\%$ are not correlated under all conditions. In a human study by Boushel and colleagues (11), a cuff was placed around the upper arm and inflated to 280 mmHg for 10 min. Then two sessions of handgrip exercises with 20 min recovery period in between were performed at 15% and 30%

maximal voluntary contraction (MVC); these were then followed by a post-exercise muscle ischemia (PEMI) period for 3 min. A correlation was seen during ischemia at rest (r = 0.6), 15% MVC handgrip (r = 0.64), 30% MVC handgrip (r = 0.56). However, NIRS-HbO_2 and O_2Hb% were not correlated during PEMI, with O_2Hb% increasing throughout the ischemic period, and NIRS-HbO_2 decreasing. According to another human study (17), NIRS-measured O_2 muscle saturation (NIRS-HbO_2) was correlated with femoral Hb saturation (femoral venous O_2Hb%) during 30-min constant workload cycling under hypoxic (r = 0.55), but not normoxic conditions. The changes in NIRS-HbO_2 and femoral venous O_2Hb% followed a parallel pattern under hypoxia. However, during exercise under normoxia, venous O_2Hb% decreased up to 15 min, and then remained stable while NIRS-HbO_2 only decreased slightly at minute 5, and then returned back to the resting level or even higher.

This correlation between NIRS signals and venous O_2Hb% has also been investigated in canine muscles at rest and during electrically stimulated muscle contractions (105). Similarly to Mancini's study (66), the difference between light absorption at 760 nm and 800 nm was used to assess Hb-Mb oxygenation. Both at rest and during electrical stimulation of the right gracilis muscle at 0.25, 0.5, 1, 2, 3, 4 and 5 Hz with supramaximal 0.5 ms pulses, a close linear correlation was observed between the NIRS signal and venous O_2Hb% (r = -0.97 $\pm$ 0.01). However, no one to date has observed the relationship between NIRS signals and O_2Hb% during hypoxia, hyperoxia, increased and decreased blood flow, and rest versus tetanic contractions in an isolated whole muscle.

II. JOURNAL MANUSCRIPT

NEAR INFRARED SPECTROSCOPY TO ASSESS THE ONSET OF INCREASED METABOLISM AND MUSCLE TISSUE OXYGENATION DURING MUSCLE CONTRACTIONS

ABSTRACT

The aims of the present study were to 1) determine whether there is a time delay (TD) in $\dot{V}O_2$ at the onset of contractions; 2) explore the contribution of myoglobin versus hemoglobin to the NIRS signals; and 3) examine the correlation between venous O_2Hb% and NIRS signals. Canine gastrocnemius muscles (GS) in six dogs were isolated and pump perfused. NIRS signals were recorded continuously and venous blood was sampled intermittently at various flow rates, with inspired gas at different O_2 fractions and during electrically stimulated muscle contractions. The myoglobin contribution to NIRS spectra was evaluated by comparing the NIRS signals under blood perfusion to the signals during hemoglobin-free Krebs-Henseleit bicarbonate buffer (KHBB) perfusion. The TD was determined from the fitting of deoxy- NIRS signals with a monoexponential model. Venous O_2Hb% was linearly correlated with deoxy-NIRS signals (R^2 = 0.93 ± 0.05) in six dogs and correlated with oxy-NIRS signals (R^2 = 0.92 ± 0.03) in five dogs. TD of HHbMb fitting was not significantly different among 1/2 s contractions with blood perfusion (8.4 ± 1.4 s), 2/3 s contractions with blood perfusion (6.5 ± 1.1) and 1/2 s contractions with KHBB perfusion (9.0 ± 2.7 s). The myoglobin contribution to NIRS signals averaged 57 ± 18% with a large inter-individual variability (39 - 83%). In conclusion, in the isolated, perfused

canine GS model, the NIRS signals reflected venous O_2Hb%; a TD still existed with KHBB perfusion, and hemoglobin and myoglobin contributed roughly equally to NIRS signals.

INTRODUCTION

At the onset of exercise, the demand for ATP increases dramatically. Although this increase in demand is often treated as a "square-wave" (20), evidence is accumulating that the initial demand at the start of contractions or exercise is significantly lower than the later steady state (1, 10, 32, 52). Regardless of the exact pattern of the increase in ATP demand, the increase in oxidative phosphorylation, which is reflected in $\dot{V}O_2$ follows an exponential model (17, 50) that is much slower. Therefore, the change in $\dot{V}O_2$ and the concomitant rate of oxidative ATP formation is not fast enough to match the O_2/ATP demand. Two classic hypotheses have been proposed to explain the relative slowness of activation of oxidative phosphorylation: 1) limitation in O_2 delivery and/or 2) requirement for activation of cellular reactions. Evidence against the O_2 delivery theory includes that the kinetics of blood flow (Q), and thereby O_2 delivery is faster than that of $\dot{V}O_2$ at exercise intensities either lower (33) or higher (8) than lactate threshold (LT). Grassi et al. (15) reported that in the isolated, perfused canine gastrocnemius complex (GS) model, convective O_2 delivery ($Q \times CaO_2$) was a limiting factor for $\dot{V}O_2$ on-kinetics during maximal intensity (15), but not submaximal intensity (13) contractions. On the other hand, Goodwin et al. (11) found that slowed blood flow kinetics (below the spontaneous level) resulted in a linear slowing of $\dot{V}O_2$ kinetics at the onset of exercise in the isolated, perfused canine GS *in situ* (11). Besides O_2 delivery, the influence of a series of metabolic factors on $\dot{V}O_2$ on-kinetics was also investigated. Studies suggested that PDH activity did not play a role in $\dot{V}O_2$ on-kinetics (2, 21, 41, 44). High [ADP] via creatine kinase (CK) inhibition (27) and observed in CK knockout mice (42) was reported to speed $\dot{V}O_2$ on-kinetics. Inhibition of nitric oxide synthase (NOS) via $_L$-NAME expedited turn-on of $\dot{V}O_2$ kinetics during

treadmill running in horses (29, 30) and during cycling in humans (24, 25), but the same effect was not found during electrically stimulated muscle contractions in the isolated, pump perfused isolated GS model (16). It is also noteworthy that the two hypotheses of O_2 delivery and metabolic activation are not mutually exclusive (49).

The typical $\dot{V}O_2$ response to exercise *in vivo* includes three phases: phase 1 ("cardiodynamic phase"), phase 2 (mono-exponential phase) and phase 3 (steady state or slow component). It is only in phase 2 that pulmonary $\dot{V}O_2$ appears to reflect muscular $\dot{V}O_2$ (43). The mono-exponential increase of $\dot{V}O_2$ in phase 2 is described by the following equation:

$$y(t) = y_{bas} + A\,[1 - e^{-(t-TD)/tau}]$$

where y_{bas} is the baseline value at rest before contractions onset; A is the amplitude between y_{bas} and the asymptote of the primary component (Phase 2); t is time; TD is the time delay, which is the time obtained from the fitting procedure and corresponds to the delay before the response becomes mono-exponential; and tau is a time constant, which is ≈63% of the time required for $\dot{V}O_2$ to rise from y_{bas} to the asymptote of the mono-exponential function. An additional parameter is MRT, which is mean response time; it is the sum of TD and tau.

Fitting of the $\dot{V}O_2$ on-kinetics with the exponential model mentioned above always includes a TD before the response becomes mono-exponential. This is true in studies of single muscle group exercise in humans (3, 22) and in isolated, perfused muscles (11, 12, 15, 19, 39) even though neither of these experimental models has a cardiodynamic component. However, whether or not there is an absolute delay in $\dot{V}O_2$ increase at exercise or contractions onset remains unsettled. Compared to studies that have focused on the changes of tau under different experimental conditions, there have been fewer studies that have directly interpreted TD. A small TD of 4.9 s – 6.1 s has been reported in studies using the isolated, perfused canine GS model (14,

15, 19). A smaller TD of 2.1 s was found in the lumbrical muscles of *Xenopus laevis* at the single muscle fiber level (28). Investigation of $\dot{V}O_2$ on-kinetics during one-legged knee-extensor exercise with human subjects revealed a TD of 3 s when blood transit time was taken into account (3). To the contrary, no TD in $\dot{V}O_2$ kinetics was found when human subjects performed 1 s duration maximal isometric ankle dorsiflexion contractions at 60 to 80-s intervals; this was determined based on modeling of the PCr recovery rate following contractions. It was also reported that no TD was found in $\dot{V}O_2$ in rat spinotrapezius muscle when $\dot{V}O_2$ was calculated from capillary red blood cell flux and microvascular PO_2 (4). Similarly, Takakura et al. (47) reported no TD when they stimulated the rat hindlimb to elicit twitch contractions; the hindlimb was perfused with Hb-free buffer and the $\dot{V}O_2$ was assessed via a near-infrared spectroscopy (NIRS) signal from muscle Mb. It appears that different techniques lead to different findings regarding TD.

NIRS is a technique that has been used extensively to noninvasively monitor muscle/brain oxygenation status at the microvascular/tissue level. The application of NIRS is based on the fact that near-infrared light (wavelength of 650 to 900 nm) can penetrate tissues to a greater depth than visible light (40). The overall light absorbance is affected by the oxygenation status of chromophore compounds such as hemoglobin (Hb) and myoglobin (Mb). Therefore, when light is emitted and received at two wavelengths, the differences in light absorbance at these two wavelengths can be used to determine the relative changes of oxygenated Hb and Mb ($HbMbO_2$) and deoxygenated Hb and Mb (HHbMb). Despite the ease of using NIRS to examine tissue oxygenation status, the method is limited in its ability to distinguish Hb signals from Mb signals.

Given that venous O_2 concentration represents the balance between $\dot{V}O_2$ and O_2 delivery and that NIRS should reveal tissue oxygenation status; one would expect a relationship between the two. The correlation between NIRS-derived signals and venous hemoglobin percent saturation with O_2 (O_2Hb%) has been investigated via comparison of jugular vein and brain measures (26), by comparing blood samples drawn from a forearm vein to NIRS spectra during an exercise of lifting weight by depressing a lever in humans (35) as well as in electrically stimulated muscle twitch contractions in rats (51) with a high correlation coefficient reported. However, this high correlation has not been observed under all conditions (6, 7).

Therefore, on the basis of the areas reviewed briefly above, the purpose of the present study in isolated, perfused canine skeletal muscle was threefold: 1) determine whether there is a TD in $\dot{V}O_2$ at contractions onset by comparing the NIRS responses during blood perfusion versus Hb-free buffer perfusion; 2) explore the contribution of Mb versus Hb to the NIRS signals; and 3) examine the correlation between venous O_2Hb% and NIRS signals under a variety of O_2 delivery and $\dot{V}O_2$ conditions.

METHODS AND PROCEDURES

Animals. All experimental procedures performed in this study were approved by the Auburn University Institutional Care and Use Committee. Six female adult mongrel hounds were used. The dogs were housed at the Division of Laboratory Animal Health facility at the Auburn University Veterinary School, with access to food and water *at libitum*. They were fasted for 24 hours before experiments.

Animal preparation. On each experimental day, one dog was anesthetized to a deep surgical plane of anesthesia. An initial bolus of sodium pentobarbital was given intravenously at 30 $mg \cdot kg^{-1}$ body weight via injection into a prominent cephalic vein of a forelimb. This

established a deep surgical plane which was maintained throughout the experiments with additional doses (65-100 mg) of sodium pentobarbital given as necessary into an isolated jugular vein to maintain absence of pedal, palpebral and corneal reflexes. An endotracheal tube was inserted into the trachea, and the dogs were ventilated with a respirator (model 613, Harvard Apparatus, Holliston, MA). Rectal temperatures were maintained at 37°C with a heating pad. Subsequent to surgical preparation, all dogs were treated with heparin in divided doses totaling 3,000 $U \cdot kg^{-1}$. Ventilation was adjusted to a level (Respirator model 613, Harvard Apparatus, Holliston, MA) that established and maintained "normal" arterial PO_2, PCO_2, and pH; initial settings were 20 $ml \cdot kg^{-1}$ body weight for tidal volume and 15-20 $breath \cdot min^{-1}$ frequency.

Surgical preparation. The left GS (gastrocnemius + superficial digital flexor) was surgically isolated as previously described (46). Briefly, a medial incision was made through the skin of the left hindlimb from midthigh to ankle. A cauterizing blade (electric soldering gun) was used to cut all of the muscles (sartorius, gracilis, semitendinosus and semimembranosus) that overlay the left GS at their insertions. With those muscles laid back, all veins (except the GS veins) that drain into the popliteal vein were ligated. The popliteal vein was cannulated, and a flow-through-type transit-time ultrasonic flow probe (6NRB440, Transonic Systems, Ithaca, NY) was placed to measure flow (Q). A reservoir was attached to a cannula in the left jugular vein. Venous blood draining from the popliteal vein was returned to the animal via the reservoir. An inline oximeter probe (Opticath Model U425C, size 4F, Hospira, Lake Forest IL) was also placed in the tubing draining the popliteal vein, as close to the muscle as possible, to measure venous $O_2Hb\%$. All the vessels from the popliteal artery that do not go to the left GS were ligated. Cotton strings were tied tightly around each head of the GS at the origins to further ensure arterial isolation. Either the right carotid artery or the right femoral artery was cannulated to

route blood through a peristaltic pump (Gilson Minipuls 3) to the GS, thus allowing experimental control of muscle perfusion. A transducer (Model RP-1500, Narco Biosystems, Austin, TX) was inserted to measure perfusion pressure to the muscle. A portion of the calcaneus, with the two tendons from the GS attached, was cut away at the heel and clamped around a metal rod for connection to an isometric myograph via a load cell (Interface SM-250, Scottsdale, AZ) and a universal joint coupler. The universal joint coupler was used to ensure that the muscle always pulled in a direct line with the load cell, without producing significant torque. The other end of the GS was left untouched. Two bone nails were used to fix the femur and tibia to the base of the myograph. A turnbuckle strut was placed parallel to the muscle between the tibial bone nail and the arm of the myograph to minimize flexing of the myograph. The sciatic nerve was exposed and isolated. The distal nerve stump was pulled into a small tubular electrode for stimulation. Saline-soaked gauze and a plastic sheet were used to cover exposed tissues to minimize drying and cooling. Prior to any experimental protocol, the GS was stimulated at a low intensity while it was progressively lengthened until a peak in force was observed; the resulting length was the optimal length (L_o) of the GS. Subsequently, the GS was re-set to this length prior to each contraction protocol.

At the end of each experiment, the left GS was removed from the animal. Surface connective tissue was carefully removed, and the muscle was weighed. The wet muscle weight was used to normalize Q and $\dot{V}O_2$. The wet muscle was then placed in an oven and dried to constant weight. The dry muscle weight was measured to determine the water percentage of the muscles. At the end of each experiment, the animal was euthanized by administering an overdose of sodium pentobarbital, along with saturated potassium chloride.

Experimental design. The experiment consisted of six trials (Trials 1, 2, 3, 4, 5 & 6) and one Pre-Trial. For Trials 1 and 2, blood flow rate via the pump was adjusted to maintain average control perfusion pressure in the range of 100-120 mmHg. Trial 1 began with the animal being respired on normoxic air. When the NIRS signals had stabilized, the blood flow was raised by increasing the pump speed by 50%. Again, when the NIRS signals were steady, the muscle blood flow was brought back to the control level. Next, the flow was decreased by 50% until the NIRS signals stabilized again. Trial 2 started with the animal ventilated on normoxic air and the control blood flow rate was maintained throughout the trial. The ventilation was then switched to 100% O_2, back to normoxic air, and then to hypoxic gas (12% O_2); the NIRS signals were allowed to stabilize during each step.

After Trials 1 and 2, a Pre-Trial for Trials 3 and 4 was performed. During this Pre-Trial, the GS was first stimulated to contract tetanically (8V, 50Hz, 0.2 ms pulse, 200ms duration) at the rate of 1 contraction per 2 s (1/2 s). Blood flow rate was adjusted with the pump to maintain average perfusion pressure around 200 mmHg; this pump setting was subsequently used in Trial 3. Without stopping contractions, the stimulation rate was then increased to 2/3 s. The pump setting was again adjusted to provide a blood flow rate that caused perfusion pressure to stabilize around 200 mmHg; this setting was subsequently used in Trial 4. Setting the pump to establish a high perfusion pressure ensured a sufficient flow rate and minimized fatigue during each trial.

The muscle was allowed to recover for 35 min, after which Trial 3 began with the GS stimulated to contract tetanically at 1/2 s for 2 min at the pre-determined flow rate. The flow rate was then increased by 20%, taken back to the control level, and decreased by 20%. The NIRS signals were allowed to stabilize at each flow rate. Following another 35 min recovery, Trial 4

was performed with a similar protocol to that of Trial 3, except that the GS was stimulated at the rate of 2/3s.

Trial 5 was done to determine the maximal range of NIRS changes with blood perfusion. First, the muscle remained at rest while the animal was ventilated on 100% O_2 with muscle blood flow rate increased by 50% above the control level; the levels of HHbMb and $HbMbO_2$ that were achieved were considered to be minimal and maximal, respectively, with blood perfusion. Next, with the animal ventilated on normoxic air, the muscle was stimulated to contract tetanically at the rate of 1/2 s with the popliteal artery clamped to stop the blood flow; the final levels of HHbMb and $HbMbO_2$ that were achieved were considered to be maximal and minimal, respectively, with blood perfusion.

For Trial 6, Krebs-Henseleit bicarbonate buffer (KHBB) was introduced into the pump line to wash all blood out of the muscle. The buffer was nominally composed of 118.5 mM NaCl, 4.75 mM KCl, 2.54 mM $CaCl_2$, 1.19 mM KH_2PO_4, 1.19 mM $MgSO_4 \cdot 7H_2O$, 25 mM $NaHCO_3$, 5 mM glucose, 1 mM NaLa and 0.1 mM NaPyr. The buffer was bubbled with 95% O_2/5% CO_2, and dextran and bovine serum albumin (BSA) were added to give concentrations of 60 $g \cdot L^{-1}$ and 1.0 $g \cdot L^{-1}$, respectively. Once the muscle venous effluent was clear of any red blood cells, the KHBB flow rate was increased until no further decrease in HHbMb was seen, suggesting that minimal HHbMb had been achieved for KHBB perfusion. The GS muscle was then stimulated to contract tetanically at 1/2 s. When the NIRS signals were no longer changing, the popliteal artery was clamped while contractions were continued to ensure complete deoxygenation of Mb.

Measurements. Outputs from the blood pressure transducer, load cell, blood flow probe, in-line oximeter probe and NIRS were connected to a computerized data-acquisition system. The sampling rate for all signals was 125 Hz for Trials 3-5 and 10 Hz for Trials 1, 2 and 6. The load

cell reaches 90% of the full response within 1 ms while the flow meter was set to its highest pulsatile cutoff frequency of 100 Hz. The load cell was calibrated with known weights before each experiment. The perfusion pump was calibrated prior to this series of experiments, and the flow probe and meter were calibrated with a graduated cylinder and clock prior to each experiment, as well as during each trial. Arterial samples were collected before and at the end of each trial for Trials 1, 3 and 4, as well as at the end of each perturbation of Trial 2. Venous samples were drawn before and after each trial for determination of PO_2, PCO_2 and pH with a blood gas, pH analyzer (GEM Premier 3000 Instrumentation Laboratory, Lexington, MA), as well as total Hb concentration and O_2Hb% via CO-Oximeter (IL-682, Instrumentation Laboratory, Lexington, MA). Venous blood was drawn from the catheter connected to the popliteal vein for calibration of the oximeter signal. Blood samples were drawn anaerobically and immediately analyzed, or capped and stored in ice water for analysis within 30 minutes.

The Oximetrix 3 sampled venous O_2Hb% at a rate of 244 samples/s, averaged the samples each second, and then gave an output of a 5-s rolling average each second. This output has a 90% response time of 5 s. The recorded data are characterized by noise, high time resolution and time delay (TD), and a response specific to the device. For this reason, the O_2Hb% recorded data were converted by sequential signal processing: filtering, deconvolution, and moving average to approximate the original raw data input signal. In particular, O_2Hb% data were filtered by Butterworth's method to attenuate the noise and reduce the high sampling time. After the filtering process, O_2Hb% data were deconvoluted by a transfer function of the first-order system to account for the characteristic TD and tau of the oximeter. Finally, the deconvoluted O_2Hb% signal was processed by a moving average second by second. Determination of the TD and tau values of the oximeter involved detecting a step decrease of

O_2Hb% using an experimental protocol whereby O_2Hb% was imposed to decrease according to a square wave function. The characteristic values of TD and tau of the oximeter were used in the transfer function of the first-order system to convert the recorded data by a deconvolution process. These procedures have been extensively detailed in previous work by our laboratory (18). $\dot{V}O_2$ of the GS with blood perfusion was calculated by the Fick relationship (equation 1): Q stands for flow rate of blood, and a-v O_2d is the difference in O_2 concentration (equation 2) between arterial and venous blood. With buffer perfusion, Fick's principle still applies. However, there is no Hb involved (equation 3).

$\dot{V}O_2$ ($ml \cdot min^{-1}$) = Q ($L \cdot min^{-1}$) × a-v O_2d ($ml \cdot L^{-1}$) ..... equation 1

a-v O_2d with blood ($ml \cdot L^{-1}$) = CaO_2 ($ml \cdot L^{-1}$) - CvO_2 ($ml \cdot L^{-1}$) = ((SaO_2% - SvO_2%) × [Hb] ($g \cdot L^{-1}$) × 1.39 ($ml \cdot g^{-1}$)) + ((PaO_2 (mmHg) – PvO_2 (mmHg)) × solubility of O_2 in blood ($ml \cdot L^{-1} \cdot mmHg^{-1}$) ..... equation 2

a-v O_2d with buffer = (PaO_2 (mmHg) – PvO_2 (mmHg)) × solubility of O_2 in buffer ($ml \cdot L^{-1} \cdot mmHg^{-1}$) ..... equation 3

Contraction-by-contraction $\dot{V}O_2$ was determined according to the Fick principle using an Excel Macro that was written in-house (18). Samples for blood flow and calculated venous O_2 concentration (from deconvoluted O_2Hb%) were averaged over each contraction cycle, allowing the calculation of $\dot{V}O_2$ on a contraction-by-contraction basis (18).

Near-infrared spectroscopy. The near-infrared spectroscopy (NIRS) system (Oxymon Mk III, Artinis Medical Systems BV, Zetten, Netherlands) was used to assess muscle oxygenation. Two fiber-optic bundles were used to emit and receive light at two different wavelengths (760 and 860 nm). The optodes were placed over the belly of the left GS and held in place with an elastic band. The muscle was covered with a dark plastic sheet throughout the

experiment to minimize interference from outside light. The two optodes were held 25 mm apart, which gave a penetration depth of about 12.5 mm (9). Relative changes in oxyhemoglobin /oxymyoglobin ($HbMbO_2$), deoxyhemoglobin/deoxymyoglobin (HHbMb) and total hemoglobin /myoglobin ($HbMb_{tot}$) were output from the system to represent the oxygenation/deoxygenation state of Hb and Mb. The NIRS signal was biased to zero at the start of each trial.

Analysis of $\dot{V}O_2$ and NIRS on-kinetics. $\dot{V}O_2$ and NIRS data were fitted with the following mono-exponential function as described earlier.

$$y_{(t)} = y_{bas} + A\,[1 - e^{-(t-TD)/tau}]$$

The onset of contractions was determined with a Microsoft Office Excel macro written in-house and data fitting was done with OriginPro 8.5 (OriginLab, One Roundhouse Plaza, Northhampton, MA). The y_{bas} was held constant as the 30 s average value prior to contractions. The other parameters (A, TD and tau) were allowed to float until the "best fit" was seen. The criteria for "best fit" have been described by Whipp et al. (23). Basically, Chi^2 and residuals of the fit, and the 95% confidence interval for tau were observed until the best combination of minimal values was achieved.

Statistical analysis. Data are presented as means ± SDs. One-way repeated-measures analysis of variance (ANOVA) was used to compare the different perturbations within each trial, as well as to compare the parameters of different trials. The level of significance was set at $p < 0.05$. If a difference was found, a Student-Newman-Keuls post-hoc test was performed to identify the locations of specific differences between pairs in the dataset. The correlations between HHbMb, $HbMbO_2$, and venous O_2Hb% were assessed with linear regression analysis.

RESULTS

Body weight and muscle weight. The average animal body weight was 15.9 ± 1.4 kg. The wet weight of the GS muscle averaged 73.8 ± 9.1 g while the dry weight was 15.4 ± 2.1 g, yielding a muscle water percentage of 79.2 ± 1.0%. The average water content was higher than observed in recent studies in our laboratory with spontaneous self-perfusion (average of 76%) likely because of perfusion with a non-blood perfusate in Trial 6. Frequent visual examination of the GS revealed no evidence of edema prior to the KHBB perfusion in Trial 6. Using 76% as the normal muscle water percentage, the adjusted wet muscle weight in the present study was 64.1 ± 9.4 g. The adjusted weights were used for normalization of Q, $\dot{V}O_2$, etc.

Trial 1 blood measures. The resting and experimental values of blood flow, blood pressure and venous O_2Hb% are displayed in Table 1. As expected, the blood flow rate at Rest and the Control Flow condition were not significantly different from each other ($p = 0.78$) but both were significantly different from High Flow ($p \leq 0.003$) and Low Flow ($p \leq 0.004$). High Flow and Low Flow were also significantly different from each other ($p < 0.0001$). A similar pattern was seen with blood pressure (perfusion pressure). Venous O_2Hb% in Low Flow was significantly lower than Rest ($p = 0.0023$), Control Flow ($p = 0.002$) and High Flow conditions ($p = 0.0009$). However, venous O_2Hb% was not significantly different among Rest, Control, and High Flow ($p \geq 0.44$).

Table 1. Blood flow, blood pressure and venous $O_2Hb\%$ in Trial 1.

	Rest	High Flow	Control Flow	Low Flow
Blood flow ($ml \cdot kg^{-1} \cdot min^{-1}$)	231 ± 108^{a}	339 ± 149^{b}	237 ± 110^{a}	133 ± 67^{c}
Blood pressure (mmHg)	140 ± 17^{a}	157 ± 17^{b}	141 ± 18^{a}	110 ± 16^{c}
Venous $O_2Hb\%$	90.9 ± 2.1^{a}	91.9 ± 1.5^{a}	91.3 ± 1.8^{a}	88.1 ± 3.6^{b}

Data are presented as means ± SD. All values with the same letter are not significantly different from each other. Values with different letters are significantly different ($p < 0.05$).

Trial 2 blood measures. The control and treatment values of PaO_2, PvO_2 and $O_2Hb\%$ in Trial 2 are shown in Table 2. The PaO_2 during Hyperoxia was significantly higher than at Rest, or in Normoxia or Hypoxia ($p < 0.0001$). Due to a greater variance in Hyperoxia, a separate repeated-measures ANOVA was run on the subset of the other three conditions. This further testing revealed that the PaO_2 values in Rest and Control were not significantly different from each other ($p = 0.56$) while PaO_2 in Hypoxia was significantly lower than these two ($P < 0.0001$). A similar pattern was seen in PvO_2. The PvO_2 in Hyperoxia was significantly higher than at Rest, in Normoxia or Hypoxia ($p \leq 0.0035$). PvO_2 at Rest and in Normoxia were not different from each other ($p = 0.088$), but both were significantly higher than during Hypoxia ($p \leq 0.017$). Venous $O_2Hb\%$ at Rest and in Normoxia were not significantly different from each other ($P = 0.40$). Venous $O_2Hb\%$ was lower in Hypoxia than the other three conditions ($P < 0.0001$) while Hyperoxia was higher than the other three ($P \leq 0.044$).

Table 2. PaO_2, PvO_2 and venous $O_2Hb\%$ in Trial 2.

	Rest	Hyperoxia	Normoxia	Hypoxia
PaO_2 (mmHg)	93 ± 9^{a}	525 ± 73^{b}	90 ± 11^{a}	45 ± 5^{c}
PvO_2 (mmHg)	70 ± 7^{a}	131 ± 44^{b}	86 ± 31^{a}	44 ± 5^{c}
Venous $O_2Hb\%$	90.7 ± 2.3^{a}	95.7 ± 1.7^{b}	92.1 ± 3.7^{a}	76.2 ± 7.3^{c}

Data are presented as means ± SD. All values with the same letter are not significantly different from each other. Values with different letters are significantly different ($p < 0.05$).

Trial 3 blood measures. The venous blood gases, blood pressure and blood flow in Trial 3 are presented in Table 3. As expected, the blood flow in Control Flow 1 and Control 2 were not significantly different from each other ($p = 0.61$), but were both significantly different from High Flow and Low Flow ($p < 0.0001$). Blood flow in High Flow and Low flow were significantly different from each other ($p < 0.0001$). The blood pressure in Control Flow 1 was significantly higher ($p = 0.0018$) than in Control Flow 2, which suggested vasodilation with muscle contractions. A significant difference was observed when perfusion pressure under Control Flow 1 was compared to Low Flow ($p < 0.0001$), but not High Flow ($p = 0.50$). The resting values of PvO_2 (84 ± 6) and CvO_2 (23.9 ± 1.7) were significantly higher than those of the four treatment conditions ($p < 0.0001$). PvO_2 and CvO_2 in Control Flow 1 were significantly higher than in Control Flow 2 with p values of 0.0012 and < 0.0001, respectively. This suggests that muscle metabolism did not reach the steady state following 2 min of muscle contractions at the rate of 1/2 s. Both High Flow and Low Flow conditions had significantly different ($p \leq 0.0001$) PvO_2 and CvO_2 from Control Flow 1. The resting venous pH was significantly higher than the four experimental conditions ($p < 0.0001$). No difference was seen in venous pH between Control Flow 1, Control Flow 2 and High Flow conditions. A significant difference was observed when venous pH in Low Flow was compared to the other three experimental conditions ($p \leq 0.0012$). Arterial parameters were measured at the beginning and end of this trial. PaO_2 was not different at the start (105 ± 22) versus the end (103 ± 23) of the trial ($p = 0.33$). The a-vO_2d was significantly higher ($p < 0.0001$) at the end (17.4 ± 3.7) of the trial compared to the resting value (0.4 ± 0.2).

Table 3. PvO_2, venous pH, CvO_2, blood pressure (BP) and blood flow in Trial 3. Control Flow 1 stands for the 2 min contractions at the beginning of the trial, and Control Flow 2 represents contractions with blood flow rate back to the control level, following the High Flow step.

	Control Flow 1	High Flow	Control Flow 2	Low Flow
Blood flow ($ml \cdot kg^{-1} \cdot min^{-1}$)	1063 ± 71^{a}	1270 ± 64^{b}	1081 ± 71^{a}	849 ± 154^{c}
PvO_2 (mmHg)	24 ± 8^{a}	26 ± 7^{c}	22 ± 8^{b}	18 ± 8^{d}
Venous pH	7.28 ± 0.04^{a}	7.28 ± 0.04^{a}	7.28 ± 0.04^{a}	7.27 ± 0.05^{c}
CvO_2 ($ml \cdot dL^{-1}$)	9.8 ± 4.9^{a}	10.9 ± 4.7^{c}	8.5 ± 5.1^{b}	6.5 ± 4.9^{d}
BP (mmHg)	188 ± 18^{a}	193 ± 17^{a}	165 ± 16^{b}	134 ± 19^{c}

Data are presented as means ± SD. All values with the same letter are not significantly different from each other. Values with different letters are significantly different ($p < 0.05$).

Trial 4 blood measures. Values for PvO_2, venous pH, CvO_2, blood pressure and blood flow are displayed in Table 4. Significant differences between all four experimental trials and the resting value were seen in PvO_2 ($p < 0.0001$), venous pH ($p < 0.0001$), CvO_2 ($p < 0.0001$) and blood pressure ($p < 0.0019$). The blood pressure in Low Flow was significantly lower than in Control Flow 1, High Flow and Control Flow 2 ($p \leq 0.0001$). Blood flow in Control Flow 1 and Control Flow 2 were not significantly different from each other ($p = 0.61$), but were significantly different from High Flow and Low Flow ($p < 0.0001$). There was no significant difference in CvO_2 between Control Flow 1 vs. Control Flow 2 ($p = 0.88$), Control Flow 1 vs. High Flow ($p = 0.72$), Control Flow 1 vs. Low Flow ($p = 0.65$) or High Flow vs. Low Flow ($p = 0.70$). PvO_2 was not significantly different among Control Flow 1, High Flow and Control Flow 2 ($p \geq 0.093$), and all three of these were significantly different from Low Flow ($p \leq 0.030$). No significant difference in venous pH was observed between Control Flow 1, High Flow and Control Flow 2 ($p \geq 0.35$), and all three of these were significantly higher than Low Flow ($p \leq 0.025$). As expected, the a-vO_2d ($p = 0.0045$) was significantly higher by the end of the trial (14.7 ± 8.0) as

compared to the start of the trial (0.1 ± 0.8). The total Hb content varied from 14.9 to 20.2 g•dL^{-1} throughout Trials 1 to 4 in the six dogs.

Table 4. PvO_2, venous pH, CvO_2, blood pressure (BP) and blood flow in Trial 4. Control Flow 1 stands for the 2 min contractions at the beginning of the trial, and Control Flow 2 represents contractions with blood flow rate back to the control level, following the High Flow step.

	Control Flow 1	High flow	Control flow 2	Low flow
Blood flow (ml•kg^{-1}•min^{-1})	1296 ± 97 ^{a}	1543 ± 109 ^{b}	1329 ± 97 ^{a}	1094 ± 92 ^{c}
PvO_2 (mmHg)	24 ± 6 ^{a}	26 ± 3 ^{a}	23 ± 6 ^{a}	20 ± 8 ^{b}
Venous pH	7.29 ± 0.03 ^{a}	7.29 ± 0.03 ^{a}	7.28 ± 0.04 ^{a}	7.27 ± 0.03 ^{b}
CvO_2 (ml•dL^{-1})	10.2 ± 4.3 ^{a}	10.8 ± 3.1 ^{a}	9.4 ± 4.5 ^{a}	9.4 ± 9 ^{a}
BP (mmHg)	204 ± 16 ^{a}	201 ± 26 ^{a}	183 ± 20 ^{a}	161 ± 37 ^{b}

Data are presented as means ± SD. All values with the same letter are not significantly different from each other. Values with different letters are significantly different ($p < 0.05$).

Trial 5. The maximal changes of HHbMb spectra in this trial were considered to reflect the maximal range of NIRS changes under blood perfusion. The average maximal HHbMb change for the six dogs was 75.8 ± 18.8 arbitrary units (au), and 136.5 ± 39.1 au for the maximal $HbMbO_2$ change.

Correlation between O_2Hb% and HHbMb. The correlations between O_2Hb% and normalized HHbMb (HHbMb%) and $HbMbO_2$ ($HbMbO_2$%) were assessed for the data collected in Trials 1-4. HHbMb% and $HbMbO_2$% were calculated by dividing HHbMb and $HbMbO_2$ in arbitrary units, by the maximal range of HHbMb and $HbMbO_2$, respectively, as determined in Trial 5. The O_2Hb% was obtained from the corresponding CO-Oximeter values measured for venous blood as described in the Methods. The HHbMb and $HbMbO_2$ values were 10 s averages of HHbMb and $HbMbO_2$ signals prior to drawing the venous sample in Trials 1 and 2; the average of the signals over the 12 s prior to the venous blood draw for Trial 3 (6 contractions) and Trial 4 (8 contractions). The 12 s time period was chosen so that average HHbMb and

$HbMbO_2$ were calculated based on NIRS changes within complete contraction cycles. The correlational relationships between O_2Hb% and HHbMb% and $HbMbO_2$% for each animal are depicted in the Figures 1 and 2. The overall relationship between O_2Hb% and HHbMb% for all animals combined is illustrated in Figure 3. The relationship between O_2Hb% and $HbMbO_2$% for Dogs 2 to 6 is illustrated in Figures 4. A high linear correlation ($R^2 = 0.93 \pm 0.05$) was seen between O_2Hb% and HHbMb% in all the six dogs. Except in Dog 1 ($R^2 = 0.27$), a high correlation between O_2Hb% and $HbMbO_2$% was observed ($R^2 = 0.92 \pm 0.03$). The two apparent outliers in Dog 1 occurred under Hypoxia and Low Flow conditions. The overall relationships between HbO_2% and HHbMb% and $HbMbO_2$% also followed a linear correlation, with R^2 of 0.75 and 0.90, respectively.

Figure 1.The correlation between HHbMb% and O_2Hb% in dogs 1-6.

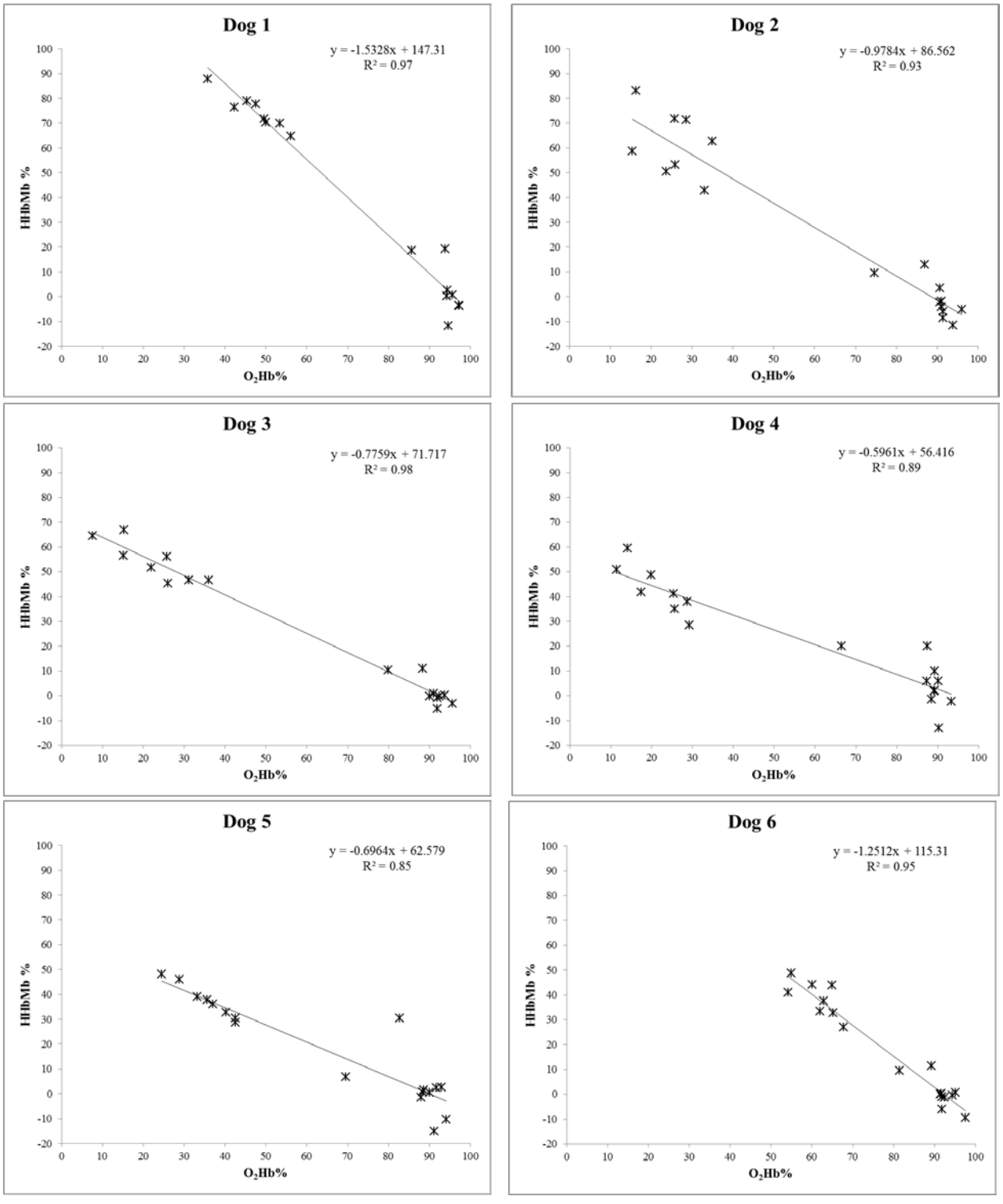

Figure 2. The correlation between $HbMbO_2$% and O_2Hb% in dogs 1-6.

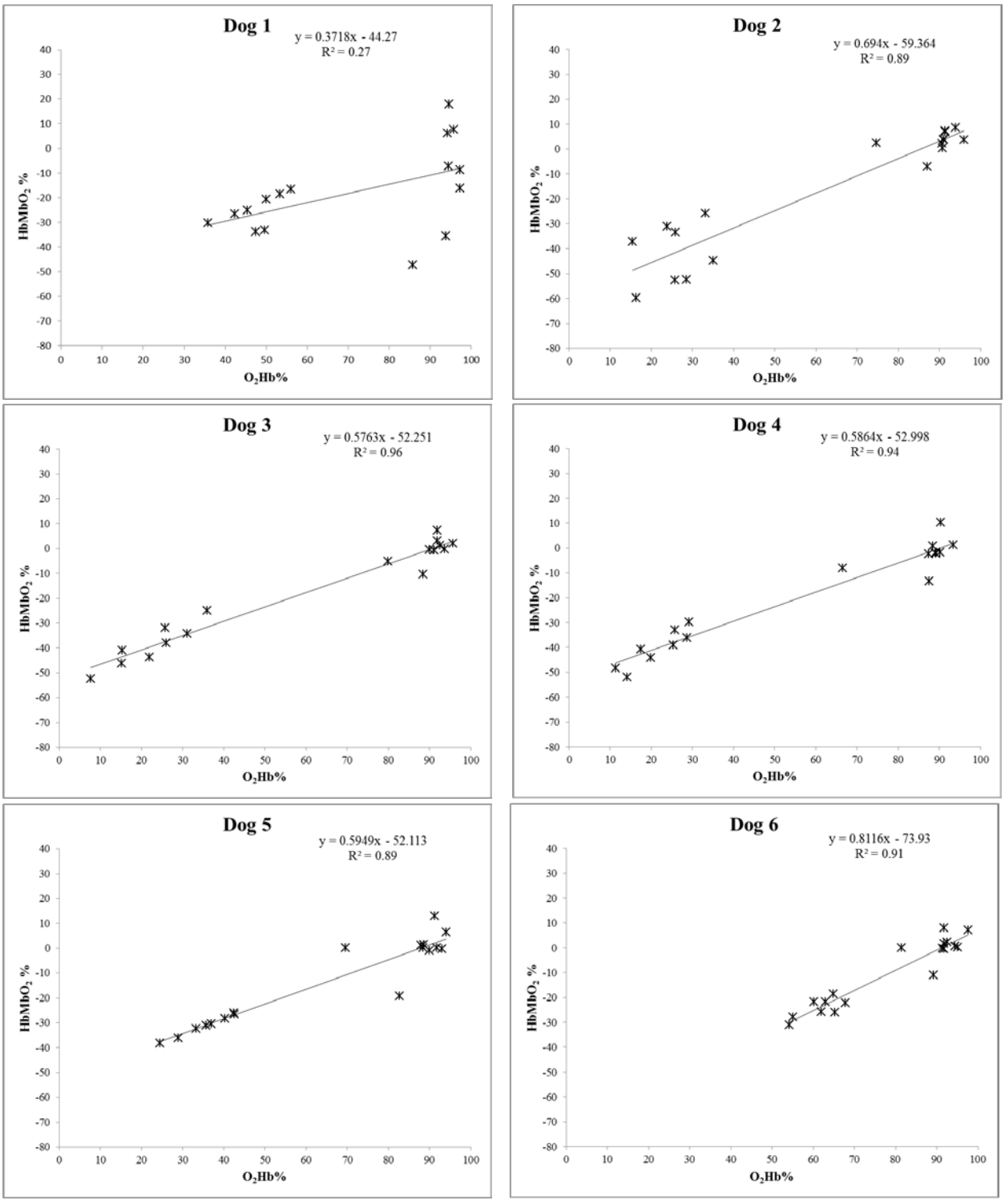

Figure 3.The overall correlation between HHbMb% and O_2Hb% in the six animals.

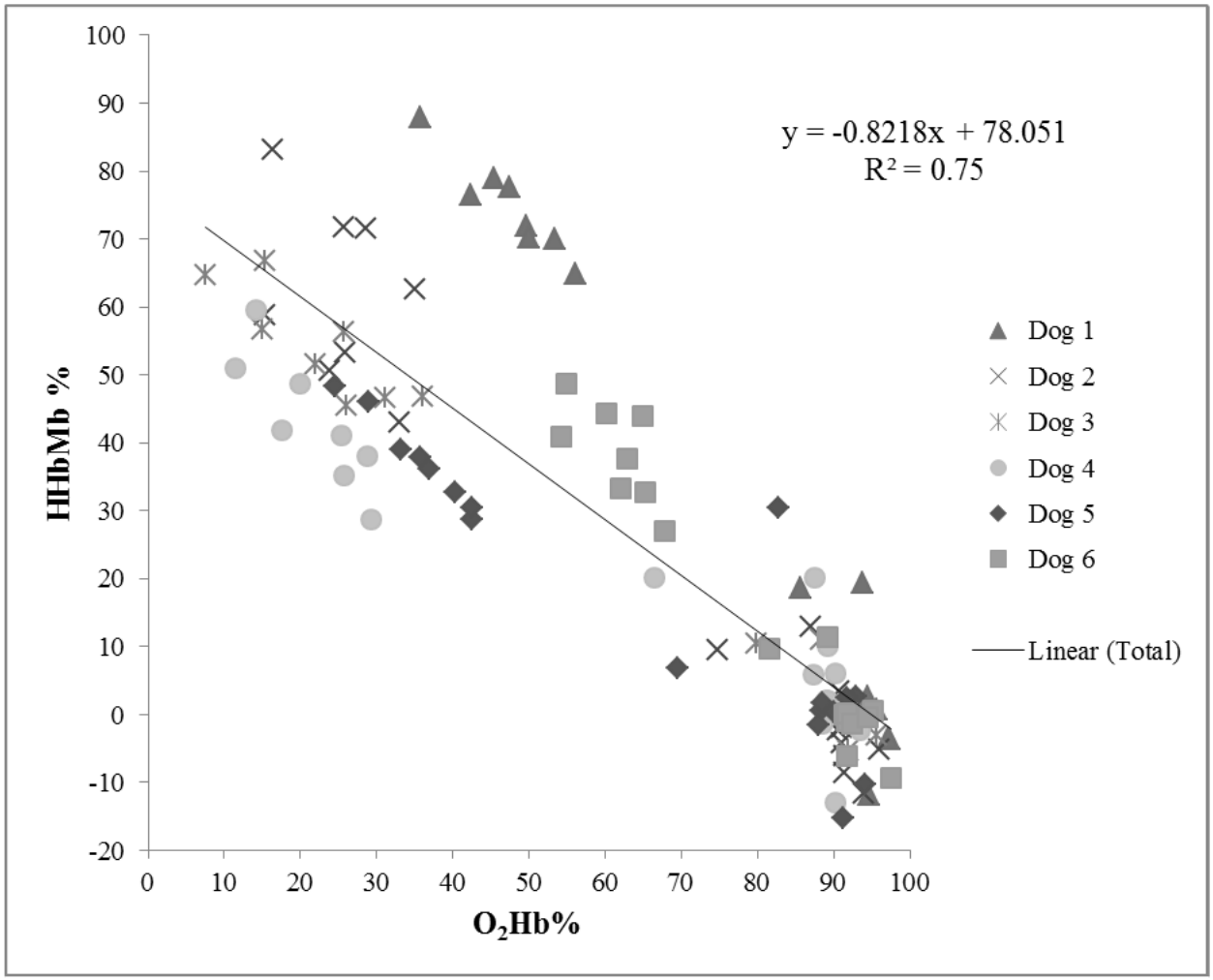

Figure 4.The overall correlation between $HbMbO_2$% and O_2Hb% in the five animals.

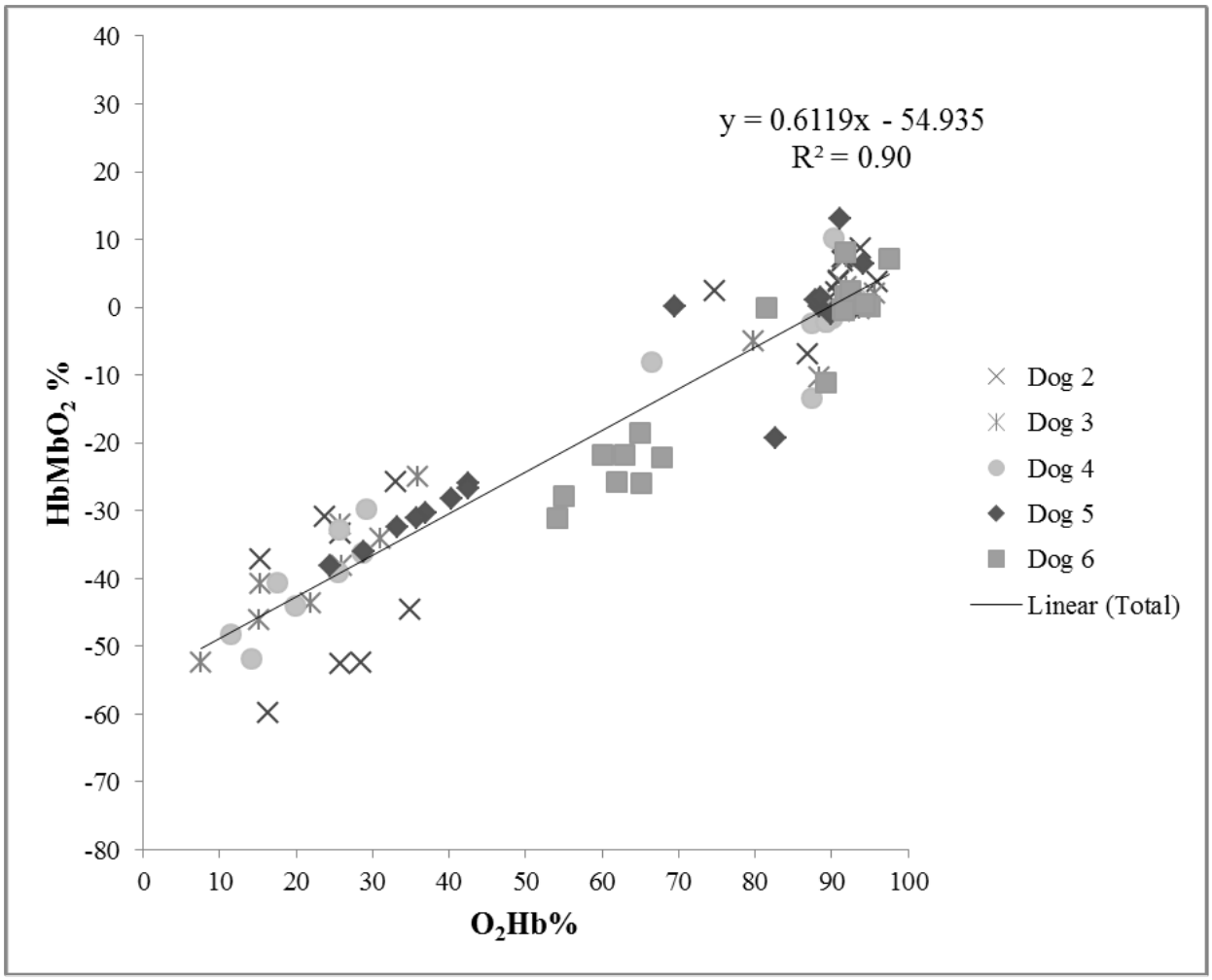

Kinetics of HHbMb. The changes of HHbMb in trials 3, 4 and 6 are depicted in Figure 5. For all experiments, the starting values (rest) for HHbMb were adjusted to zero to facilitate the comparisons between the three trials. The on-kinetics of HHbMb is shown in Table 5. No significant difference was observed in TD, amplitude, asymptote or slow component among the three trials. The tau of Trial 6 was significantly lower than in Trials 3 ($p = 0.0071$) and 4 ($p = 0.007$). A significantly shorter MRT was seen in Trial 6, compared to Trial 3 ($p = 0.015$).

The typical changes of $HbMbO_2$, HHbMb and $HbMb_{tot}$ during the first few contractions in Trials 3 and 6 are illustrated in Figure 6. An initial decrease was observed at the onset of each contraction cycle with both blood and KHBB perfusion. In the event that this decrease might be

an artifact, a separate analysis (Macro 2) was done; in this analysis, only the NIRS data in the "recovery" period of each contraction cycle were used. The fitting parameters from this analysis were compared to the results in which all of the data (including the initial decrease) were analyzed (Macro 1); see Table 5. No significant difference was observed in TD ($p \geq 0.061$), tau ($p \geq 0.091$) and MRT ($p \geq 0.11$) in Trials 3 and 6. The TD and tau from Macro 1 was significantly higher ($p = 0.027$) and lower ($p = 0.0052$) than from Macro 2, respectively while the MRT was not significantly different between Macro 1 and Macro 2 ($p = 0.91$) in Trial 4. As expected, a higher asymptote ($p \leq 0.0034$) and amplitude ($p \leq 0.0032$) was observed from Macro 2 as compared to Macro 1.

Table 5.The kinetics of HHbMb in Trials 3, 4 and 6.

	Trial 3		Trial 4		Trial 6	
	Macro 1	Macro 2	Macro 1	Macro 2	Macro 1	Macro 2
TD (s)	8.4 ± 1.4	8.0 ± 1.4	6.5 ± 1.1 *	5.9 ± 0.9 *	9.0 ± 2.7	9.0 ± 2.8
tau (s)	7.2 ± 2.6 [c]	7.0 ± 2.5	7.7 ± 3.7 [b]*	8.3 ± 3.9 *	4.1 ± 1.2 [bc]	3.8 ± 1.0
MRT (s)	15.5 ± 2.1 [c]	15.0 ± 2.1	14.2 ± 3.9	14.3 ± 4.0	13.0 ± 3.6 [c]	12.8 ± 3.5
Amplitude	28.2 ± 7.4 *	29.8 ± 7.7 *	31.7 ± 6.8 *	33.8 ± 7.5 *	31.8 ± 5.8 *	34.5 ± 6.4 *
Asymptote	28.4 ± 7.4 *	30.0 ± 7.7*	31.3 ± 6.7 *	33.4 ± 7.4 *	36.4 ± 13.8 *	39.1 ± 14.5 *
Slow component	4.3 ± 5.5	4.7 ± 5.5	4.7 ± 5.7	3.8 ± 5.2	0.3 ± 1.8	0.5 ± 1.3

Data are presented as means ± SD. [a] indicates significant difference ($p<0.05$) between Trial 3 and Trial 4. [b] indicates significant difference between Trial 4 and Trial 6. [c] indicates significant difference between Trial 3 and Trial 6. * indicates significant difference between Macro1 and Macro 2.

Figure 5. The changes of HHbMb% (HHbMb standardized by maximal HHbMb changes determined in Trial 5) in Trials 3, 4 and 6.The solid square data points and solid fitting line stand for Trial 3; hollow triangle data points and dash fitting line are for Trial 4; hollow round data points and dot fitting line represent Trial 6.

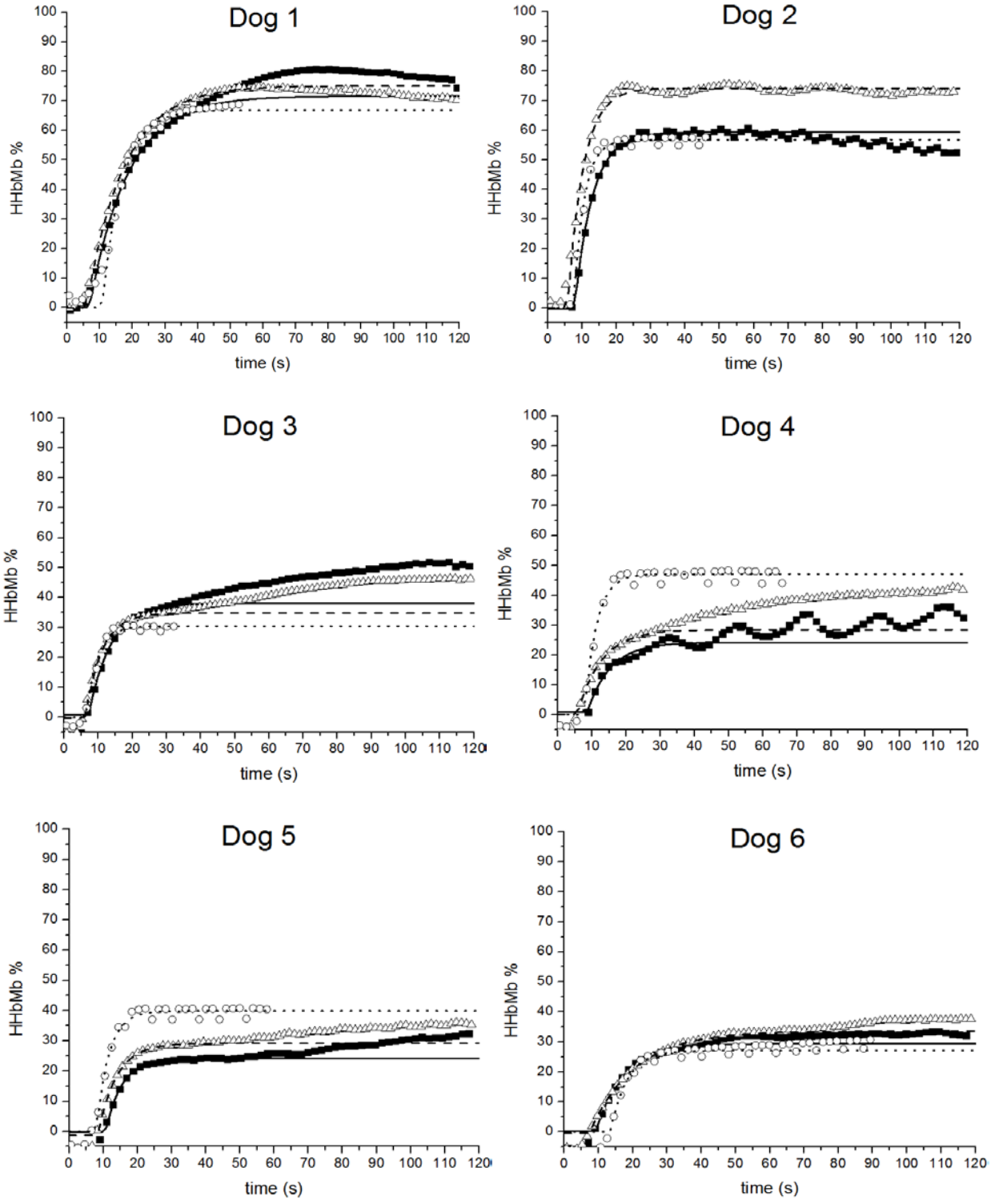

Figure 6. Typical NIRS changes during muscle contractions (Dog #3). The upper three panels illustrate $HbMbO_2$, HHbMb and $HbMb_{tot}$ changes during Trial 3 (1/2 s contractions during blood perfusion). The middle three panels display MbO_2, HMb and Mb_{tot} changes during Trial 6 (1/2 s contractions during KHBB perfusion). The lower panel illustrates the period of contractions selected by Macro1 and Macro 2 for data fitting.

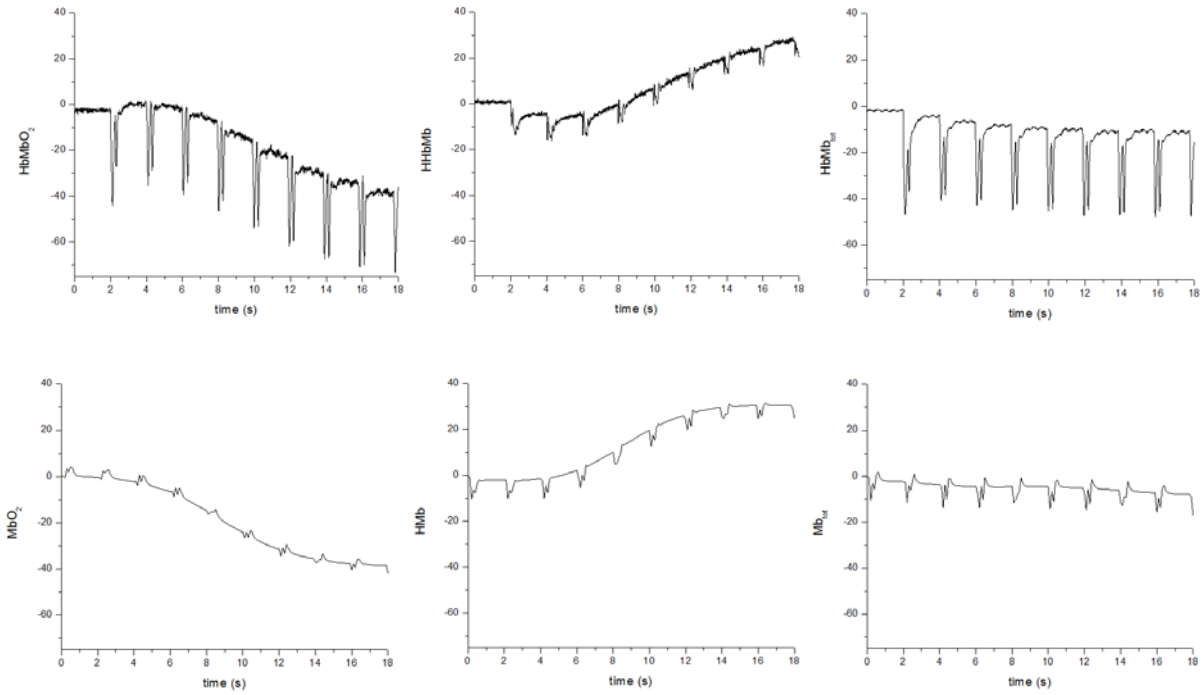

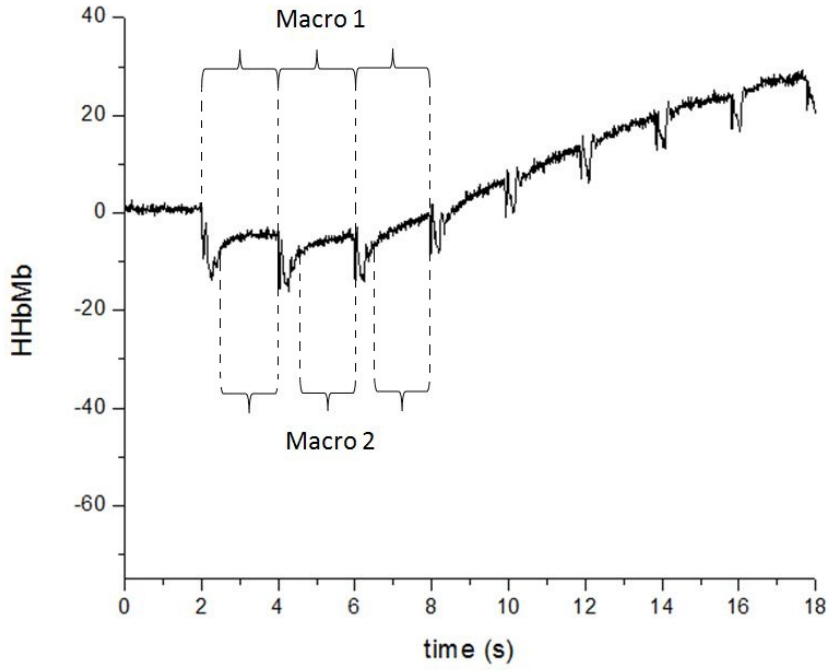

Kinetics of $\dot{V}O_2$. It was only possible to measure $\dot{V}O_2$ in trials 3 and 4. The information is presented in Table 6 and illustrated in Figure 7. A significant difference existed between Trial 3 and 4 in TD ($p = 0.019$), amplitude ($p = 0.0026$) and asymptote ($p = 0.0058$). The TD of Trial 4 was slightly, but significantly lower than Trial 3, while, as expected, the amplitude and asymptote of $\dot{V}O_2$ in Trial 4 were higher than in Trial 3. Tau, MRT, baseline $\dot{V}O_2$ and slow component were not significantly different between the two trials. The TD, tau and MRT of the kinetics of HHbMb and $\dot{V}O_2$ were not significantly different from each other in Trial 3 ($p \geq 0.052$) and Trial 4 ($p \geq 0.24$).

Table 6. The kinetics of $\dot{V}O_2$ in trials 3 and 4.

	Trial 3	Trial 4
TD (s)	7.4 ± 0.7	6.4 ± 1.1 [a]
tau (s)	9.9 ± 1.3	10.3 ± 2.3
MRT (s)	17.3 ± 1.7	16.7 ± 2.0
Baseline $\dot{V}O_2$ ($ml \cdot kg^{-1} \cdot min^{-1}$)	6.2 ± 2.2	9.6 ± 5.4
Amplitude ($ml \cdot kg^{-1} \cdot min^{-1}$)	119.3 ± 31.6	145.4 ± 40.2 [a]
Asymptote ($ml \cdot kg^{-1} \cdot min^{-1}$)	125.5 ± 33.2	155 ± 44.7 [a]
Slow component ($ml \cdot kg^{-1} \cdot min^{-1}$)	31.6 ± 10.8	33.5 ± 17.7

Data are presented as means ± SD. [a] indicates significant difference ($p<0.05$) between Trial 3 (one contraction per 2 s) and Trial 4 (2 contractions per 3 s).

Figure 7. The kinetics of $\dot{V}O_2$ in Trials 3 and 4. Solid square data points and solid fitting line stand for Trial 3, and hollow triangle data points and dash fitting line are for Trial 4.

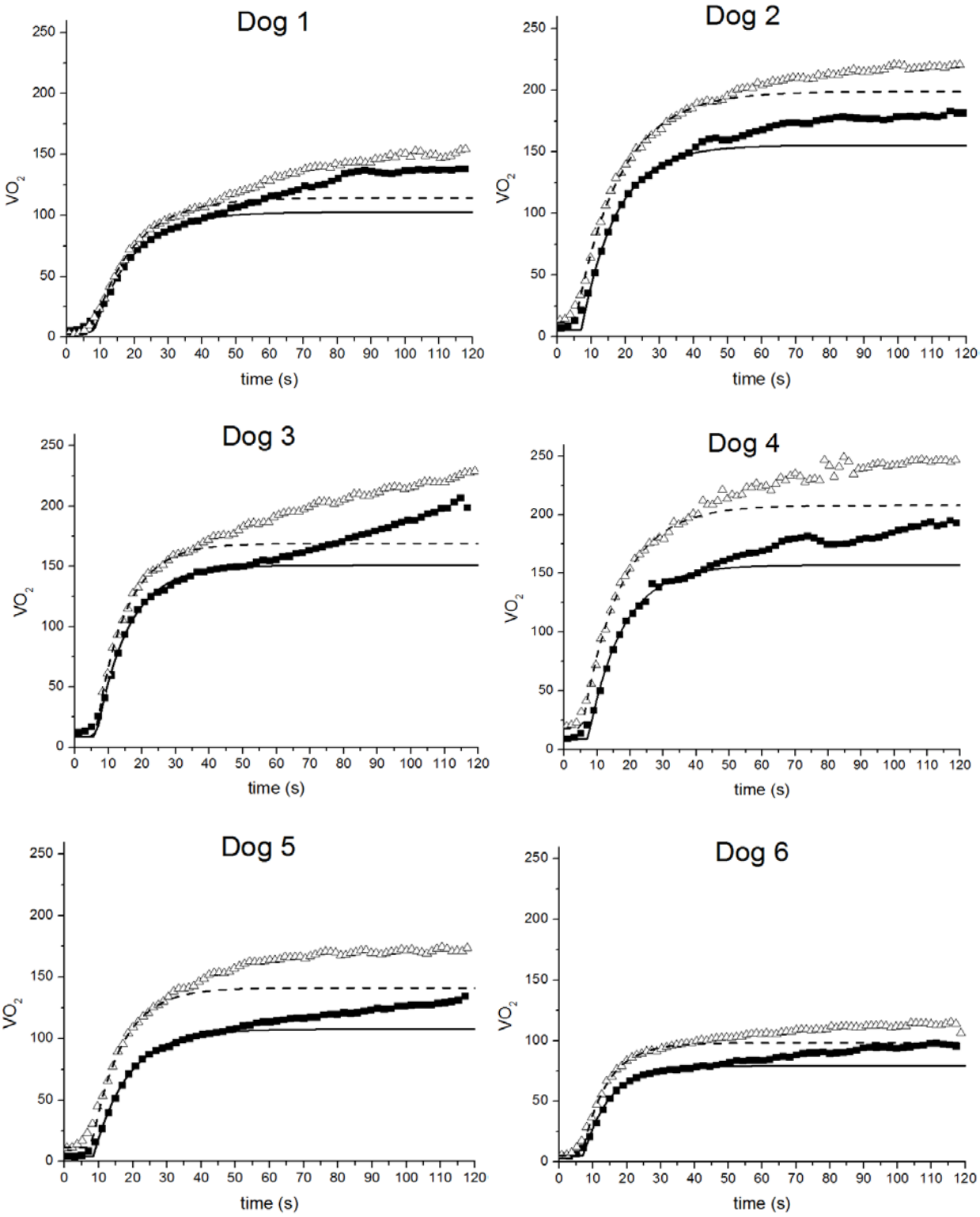

KHBB. A venous sample was drawn at rest prior to the onset of contractions in Trial 6 to confirm that the GS muscle was sufficiently supplied with O_2. This PvO_2 for the six animals averaged 188 ± 45 mmHg. A flow calibration showed that the buffer flow rate was 927 ± 272 $ml \cdot min^{-1} \cdot kg^{-1}$. A sample of Krebs buffer was measured at the end of the trial. The results were as follows: PO_2 513 ± 52 mmHg; PCO_2 36 ± 3 mmHg; pH 7.40 ± 0.03; Na^+ 150 ± 1 mM; K^+ 5.4 ± 0.1 mM; Ca^{2+} 2.01 ± 0.06 mM; Glucose 83 ± 7 $mg \cdot dL^{-1}$; La 0.7 ± 0.2 mM, and HCO_3^- 24.8 ± 1.0 mM. The average maximal range of HMb changes for the six dogs was 40.6 ± 5.1 au.

DISCUSSION

Major findings. The major findings of the present study are: 1) A high correlation existed between HHbMb and O_2Hb% for all the six animals, and between $HbMbO_2$ and O_2Hb% for five out of the six animals under a variety of inspired gas conditions, and with different blood flows both at rest and at different intensities of muscle contractions; 2) At least part of the NIRS signal during the force production portion of a muscle contraction appears to be an artifact; 3) The relative contribution of Mb to NIRS signal cannot be determined by comparing the NIRS changes during blood perfusion to those during perfusion with a buffer containing no Hb; and 4) An average TD of 9.0 s was still observed during 1/2s electrically stimulated muscle contractions during perfusion with Hb-free buffer, a value not significantly different ($p = 0.62$) from the same type of contractions under normal blood perfusion.

NIRS correlation with venous O_2Hb%. The relationship between HHbMb/$HbMbO_2$ and venous O_2Hb% was evaluated under four conditions in each of Trials 1 and 2, and five conditions each in Trials 3 and 4. To our knowledge, this is the first study to evaluate the correlation between O_2Hb% and the NIRS signals during such a wide variety of physiological conditions (normoxia, hyperoxia, and hypoxia, as well as various blood flow rates, both at rest

and during muscle contractions of differing metabolic intensity). It is expected that $HbMb_{tot}$ would affect the correlation between venous $O_2Hb\%$ and the absolute value of NIRS measurements (31, 54). For example, jugular venous bulb O_2 saturation (jugular venous $O_2Hb\%$) was measured and compared to NIRS-measured cerebral oxygenation during surgical operations in humans 10 min after the start of the operation, after 400ml blood loss, after 800ml blood loss and right before blood transfusion (54). In that study (54), absolute NIRS values did not change in parallel with O_2 saturation in the jugular venous sample. Instead, jugular venous $O_2Hb\%$ remained unchanged with decreases in $HbMb_{tot}$ whereas NIRS values decreased significantly. Therefore, in the present study, the influence of various $HbMb_{tot}$ concentrations in different animals ([Hb] in the range of 14.9 to 20.2 $g \bullet dL^{-1}$) was hopefully minimized by normalizing NIRS measurements to the maximal range of NIRS changes. However, in spite of normalization of the NIRS signal, we still observed inter-individual variability in that the overall correlation of HHbMb% with venous $O_2Hb\%$ in the combined data of the six animals displayed a weaker relationship (See Figure 3; $R^2 = 0.75$) in comparison to the relationship within each individual subject (See Figure 1; $R^2 = 0.85 - 0.98$). A study similar to the present one was conducted by Wilson et al. (51). In their study, the right canine gracilis muscle was isolated and electrically stimulated to elicit twitch contractions at 0.25, 0.5, 1, 2, 3, 4 and 5 Hz. A high linear correlation was observed between HHbMb and venous $O_2Hb\%$ ($R = -0.97 \pm 0.01$). Similar to the present study, an inter-individual variability in the slope and intercept of the correlation curve was observed. Therefore, our present study confirmed and extended the results of Wilson et al. (51). Overall, these results suggest that for a particular subject/muscle, the deoxy-/oxy- NIRS signals reflect the O_2 level of the tissue's venous drainage under a wide variety of physiological conditions.

The relationship between $O_2Hb\%$ and $HHbMb/HbMbO_2$ has also been investigated in humans *in vivo*. A cerebral oximeter is a NIRS-based device that has been used intensively in clinical settings to monitor brain oxygenation (9). Jugular venous $O_2Hb\%$ determined from blood samples was reported to be linearly correlated ($R^2 = 0.90 \pm 0.09$) with cerebral-oximeter-measured HbO_2 saturation under hypercapnic/hypoxic and normocapnic/hypoxic conditions (26). In another study by Mancini et al. (35), venous $O_2Hb\%$ and the deoxy-NIRS signal in deep arm muscles were also compared during an exercise of depressing a lever that lifted a weight every 4 s for 2 min. In this study (35), when a blood pressure cuff was placed around the upper arm and inflated to over 200 mmHg, the observed NIRS spectra at the endpoint of occlusion were considered to represent maximal Hb/Mb deoxygenation. The NIRS signal following the release of the cuff was considered to reflect maximal Hb/Mb oxygenation. The maximal range of NIRS changes was used to normalize changes in deoxygenation during contractions. A high correlation ($R^2 = 0.92 \pm 0.02$) was observed between HHbMb and venous $O_2Hb\%$. Other evidence suggested that the oxy-NIRS signal ($HbMbO_2$) and venous $O_2Hb\%$ were not correlated under all conditions. In a human study by Boushel and colleagues (6), a cuff was first placed around the upper arm and inflated to 280 mmHg for 10 min while venous blood samples were drawn every minute. Then the cuff was deflated and two sessions of handgrip exercises were performed at 15% and 30% maximal voluntary contraction with 20 min recovery period in between; these were then followed by a post-exercise muscle ischemia (PEMI) period for 3 min. A correlation was seen during ischemia at rest ($r = 0.6$), 15% MVC handgrip ($r = 0.64$) and 30% MVC handgrip ($r = 0.56$). However, $HbMbO_2$ and $O_2Hb\%$ were not correlated during PEMI, with $O_2Hb\%$ increasing throughout the ischemic period, and NIRS-HbO_2 decreasing. Finally, Costes et al. (7) reported that NIRS-measured O_2 muscle saturation (NIRS-$O_2Hb\%$) was correlated with femoral

HbO_2 saturation (femoral venous O_2Hb%) during 30 min of constant workload cycling under normoxic (r = 0.55), but not hypoxic conditions. The changes in NIRS-O_2Hb% and femoral venous O_2Hb% followed a parallel pattern under hypoxia. However, during exercise under normoxia, venous O_2Hb% decreased up to 15 min, and then remained stable while NIRS- O_2Hb% only decreased slightly at minute 5, and then returned back to the resting level or even higher.

It is noteworthy that with regard to examining the correlation between O_2Hb% and NIRS measurements, the isolated perfused canine GS model is superior to human studies in two ways. Firstly, the depth of tissue that near infrared light can penetrate into is about 1.5 cm (9) to 2-6 cm (5). Therefore, excessive subcutaneous fat would make NIRS interrogation less effective or even impossible in detecting tissue oxygenation status. Secondly, venous O_2Hb% measured from blood samples in human studies *in vivo* reflect the oxygenation status of the mixture of venous blood draining local tissues. For example, in the study by Mancini et al. (35), even though the catheter was inserted deep into the vein in order to collect blood that was primarily from exercising muscles, the authors were still only able to conclude that the collected blood originated partly from the target muscle. However, the application of our results is that for an individual muscle or perhaps muscle group, NIRS HHbMb and $HbMbO_2$ signals should reflect the mean venous O_2 saturation within the limits to which the NIRS signals are derived primarily from the muscle in question. One limitation of our results is that blood flow was not spontaneous, but was controlled by a pump; albeit one could argue that this was an advantage from an experimental viewpoint.

NIRS signals during contractions. As mentioned earlier, a decrease in $HbMbO_2$, HHbMb and $HbMb_{tot}$ was observed at the onset of each contraction cycle during the 1/2 s (see upper three panels of Figure 6), and the 2/3 s muscle contractions under blood perfusion. This

decrease has typically been ascribed to the expulsion of blood during the force production phase of a contraction cycle. Since Hb would be squeezed out of the region being monitored by NIRS, it made sense that the absorption spectra of deoxy-, oxy- and total NIRS signals would decrease as observed experimentally. However, surprisingly, a similar pattern of NIRS changes were seen in Trial 6 (muscle contractions under KHBB perfusion) in the present study; both HMb and Mb_{tot} decreased during the initial ~0.2 s of each contraction, while MbO_2 fluctuated within a small range. Since there was no Hb in the KHBB, and Mb content should not change within each contraction cycle, it appears that the changes in the NIRS signal during actual force production were an artifact. Therefore, at least part of the NIRS fluctuation at the beginning of each contraction cycle is apparently not representative of real physiological phenomena. Our hypothesis is that the actual contraction of the muscle during force production causes a change in the effective pathlength between the NIRS optodes, resulting in the observed artifact. With comparison of the fitting parameters from Macro 2 (based on "recovery" period) and Macro 1 (based on the entire contraction cycle), our data showed that including the initial period (~0.6s) of muscle contractions in the data fitting did not make a difference in TD, tau and MRT at 1/2s contractions with either blood perfusion or KHBB perfusion. However, data processing only based on the "recovery" period of contractions yielded a shorter TD and a longer tau at 2/3s contractions under blood perfusion. In all cases, a smaller amplitude and asymptote of HHbMb was observed when analyzed with Macro 2. Therefore, researchers should take caution in future studies when analyzing NIRS signals during muscle contractions. We think the safer option is to analyze only the between-contraction portion of the signals.

Mb contribution to the NIRS signal. As mentioned earlier, one of the limitations of most NIRS devices is that they cannot distinguish the separate contributions of Mb versus Hb to the

absorption spectra. The reason is that NIRS detects heme groups, and their oxygenation /deoxygenation status in both Hb and Mb (38). Seiyama et al. (45) reported that the contribution of Mb to the NIRS signal was less than 10% by comparing the absorption spectra of isolated, perfused rat hindlimbs during perfusion with blood versus perfusion with fluorocarbon under various conditions. They (45) also found a linear relationship between Hb concentration and light absorbance with hematocrit varying from 15% to 50%. Mancini's group (35) also investigated this issue with ^{1}H-magnetic resonance spectroscopy (MRS) and NIRS. In their study (35), supine plantar flexion at maximal workload was performed for 3 min, which was followed by pneumatic cuffing of the thigh. MRS showed no trace of HMb in spite of 80% deoxygenation detected by NIRS throughout the experiments in three out of the four subjects. In the fourth subject, an HMb signal was found with 5 min of ischemia from cuffing. Therefore, it was concluded that the NIRS signal was almost completely derived from Hb during exercise. However, Tran et al. (48) reached an opposite conclusion using the same technique. In Tran's study (48), MRS and NIRS signals were continuously collected during pressure cuffing of a leg for 10 min. Both MRS (Mb) and NIRS (Hb + Mb) followed similar time courses in response to cuffing, suggesting that Mb was the major contributor to the NIRS signal. The same question has also been investigated with a mathematical model, based on experimental data from humans performing moderate exercise on a cycle ergometer under normoxic and hypoxic conditions (34). This modeling suggested that the Mb contribution to the NIRS spectra was in the range of 30-35%.

A study design similar to that of the present study was used by Masuda et al. (36) in a rat hindlimb preparation. The sciatic nerve was electrically stimulated to elicit twitch contractions. The NIRS amplitude was compared between periods of autologous perfusion (blood) and Krebs

buffer perfusion, and it appeared that Mb made a contribution of about 50% to the overall NIRS signal at the intensity eliciting 50% of maximal twitch tension. However, the Mb contribution to NIRS signal at 100% twitch tension was not reported. In the present study, we attempted to determine the contribution of Mb to the NIRS spectra by comparing the maximal changes of HHbMb in Trials 5 (blood perfusion) and 6 (KHBB perfusion). The maximal range of absolute HHbMb and HMb changes was 75.8 ± 18.8 and 40.6 ± 5.1 for Trials 5 and 6, respectively. The contribution of Mb was calculated by dividing the Mb-only range by the Mb + Hb range; the average was 57 ± 18%. The major concern with the Masuda study (36) is that twitch contractions were elicited instead of tetanic contractions. According to another study by the same group (47), even the $\dot{V}O_2$ measured at maximal twitch tension (0.69 μmol·g^{-1}·min^{-1}) was less than twice as high as the resting value (0.46 μmol·g^{-1}·min^{-1}). In conclusion, our data suggest that the maximal contribution of Mb to the NIRS signal is on the order of 55-60%. However, it should be emphasized that there is considerable variability in this estimate; as Table 7 shows, the range of Mb contribution was from 39 to 83%. Also, we consider this to be a maximal estimation because it seems likely that the optical pathlength would change in going from blood perfusion to Hb-free perfusion. The scattering and absorption of light is largely affected by tissue content, including Hb. When blood was washed out and replaced by Hb-free buffer, the pathlength of light could have been altered in a manner that exaggerated the Mb contribution. This emphasizes the point that our estimate of the Mb component of typical NIRS measures is a maximal estimate, and also calls into question the notion that Hb-free solutions can provide a criterion measure of the Mb contribution.

Table 7. The maximal ranges of NIRS changes in Trial 5 (blood perfusion; HHbMb signal) and Trial 6 (KHBB perfusion; Mb-only signal), as well as a percentage comparison of the two.

Dog #	Trial 5 (blood)		Trial 6 (KHBB)		Change in Trial 5 (blood)	Change in Trial 6 (KHBB)	Percentage (KHBB/blood)
	Rest	Max	Rest	Max			
1	-4.2	44.2	-7.6	32.6	48.4	40.2	83
2	16.5	73.0	-9.9	32.0	56.5	41.9	74
3	-6.6	89.6	-0.09	39.6	96.2	39.7	41
4	-12.0	74.2	15.9	64.6	86.2	48.7	56
5	-10.7	72.7	15.8	56.4	83.4	40.6	49
6	-5.7	78.2	13.6	46.2	83.9	32.6	39

TD for increase in oxygen consumption. First, it is important to note that the responses of $\dot{V}O_2$ on-kinetics in the present study were similar to those observed in previous studies using this same canine model; Table 6 illustrates those responses. In particular, note that in all cases, the monoexponential fit for the primary or fundamental $\dot{V}O_2$ response resulted in a TD as reported in previous studies (14, 15, 19). Despite this result, however, an initial increase in $\dot{V}O_2$ was observed within the time frame of TD, as illustrated in Figure 7. A similar pattern was also found by Wüst et al. (53), who suggested that a different fitting model might better characterize the muscular $\dot{V}O_2$ responses at the onset of contractions (52).

More germane to the present investigation, however, is whether or not there is a "true" time delay in the onset of O_2 consumption within the muscle itself. It is of course possible that the reported TD is due to the transit time of blood from muscle fibers (where metabolism happens) to the vein exiting the muscle (where $\dot{V}O_2$ is actually measured). Therefore, the NIRS signals, in particular HHbMb, have been investigated in an attempt to gain insight from events that are occurring inside the muscle tissue as opposed to closely outside the muscle. However, fitting of the HHbMb signal reveals a TD that is similar to that for $\dot{V}O_2$; this could be due to the

fact that O_2 utilization is temporarily matched by O_2 delivery at contractions onset. The O_2 delivery is derived from blood flow delivering O_2 bound to Hb at contractions onset.

Therefore, we hypothesized that replacing blood perfusion with Hb-free KHBB perfusion would decrease the TD to a minimal level. However, the TD with KHBB perfusion (9.0 ± 2.7 s) was not significantly shorter than the TD for either Trial 3 (8.4 ± 1.4 s) or Trial 4 (6.5 ± 1.1 s). This means that either dissolved O_2 within the muscle tissue temporarily buffered changes in MbO_2 to HMb, or the consistently observed TD is "real" and is due to metabolic control.

Therefore, we estimated the dissolved O_2 stores within the muscle. Since the GS muscle is about 76% water, this means that 1 kg of muscle contains about 760 ml of water. Assuming that 1) the tissue water has the same O_2 solubility as the KHBB (which is equal to O_2 solubility in plasma; 0.000031578 ml $O_2 \cdot$ml fluid$^{-1} \cdot$mmHg^{-1}), 2) tissue PO_2 is approximated by PvO_2, and 3) Mb will begin to desaturate at a PO_2 of approximately 40 mmHg; the calculations for dissolved O_2 content are as follows:

$$760 \text{ml} \cdot \text{kg}^{-1} \text{ muscle} \times 0.000031578 \text{ ml } O_2 \cdot \text{ml}^{-1} \cdot \text{mmHg}^{-1} \times (PvO_2 \text{ @ rest} - 40 \text{ mmHg})$$

The value of 40 mmHg for the onset of O_2 dissociation from Mb is based on the dissociation curve of Mb, which is illustrated in Figure 8.

Figure 8. The dissociation curves of Hb and Mb, modified from Horton et al. 1996, "Principles of Biochemistry", Prentice Hall.

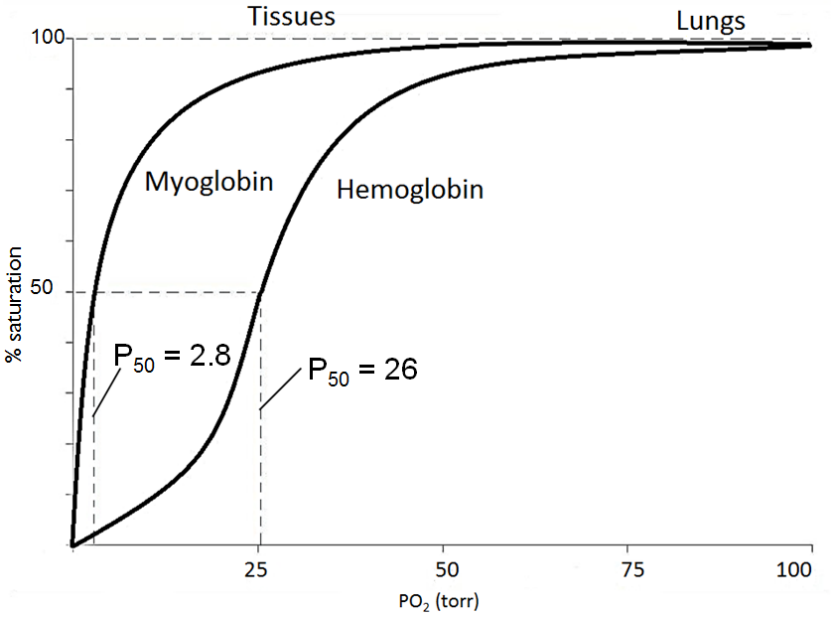

Besides dissolved O_2, another source of O_2 is the dynamic supply from buffer flow. Again, assuming than O_2 began to dissociate from Mb at a PvO_2 of 40 mmHg, and that PaO_2 was held constant, the O_2 supply from buffer flow is estimated as:

$$\text{Flow rate } (ml \cdot kg^{-1} \cdot min^{-1}) \times 0.000031578 \text{ ml } O_2 \cdot ml^{-1} \cdot mmHg^{-1} \times (PaO_2 - 40 \text{ mmHg})$$

It was lastly assumed that oxygen consumption at contractions onset increased in a manner that was the same as in Trial 3, but without any TD. Therefore, the $\dot{V}O_2$ response was:

$$y_{(t)} = y_{bas} + A\,[1 - e^{-(t)/tau}]$$

Based on the assumptions above, the TD of HMb in Trial 6 could be partially explained by the time that dissolved O_2 and O_2 from buffer flow were sufficient to match O_2 consumption. The data are listed in Table 8.

Table 8. The TD of HMb in Trial 6, and the calculated time for depletion of O_2 supply at contractions onset.

Dog #	TD (s)	Time for depletion of O_2 supply (s)
1	10.7	9.5
2	7.5	6.3
3	6.2	4.5
4	7.8	6.8
5	8.0	8.2
6	13.5	11.6
Average ± SD	9.0 ± 2.7	7.3 ± 2.4

Therefore, these data support the idea that there is no actual delay in the increase in oxidative phosphorylation, and thereby $\dot{V}O_2$ at contractions onset. This does not preclude the possibility that other models besides a monoexponential may be a more accurate representation of the overall $\dot{V}O_2$ on-kinetics.

Limitations. There are several limitations of the present study. Firstly, the canine GS muscle is highly oxidative, almost exclusively made up of type S (oxidative) and type FR (oxidative/glycolytic) muscle fibers (37). Therefore, the findings of the present study need to be interpreted with caution, especially when applied to other species or more glycolytic muscle groups. The blood flow in this study was pump controlled. This allows us to investigate the correlation between NIRS signals and venous O_2Hb% at various controlled flow rates, not spontaneously regulated flow as observed during exercise. In addition, the canine GS model induced isometric muscle contractions via electrical stimulation of the sciatic nerve. In this type of contraction, all the motor units are recruited simultaneously, which is different from the recruitment pattern of other exercise. Finally, Oxymon was the only NIRS instrument we used, so it is possible that instruments from other manufacturers could give different results.

Conclusions. In conclusion, a linear correlation between HHbMb, $HbMbO_2$ and venous O_2Hb% for individual subjects/muscles was confirmed under various blood flows, various

inspired O_2 percentages, and at two different intensities of muscle contractions. During Hb-free perfusion, changes in the NIRS signals during the force production phase of the contraction cycle persisted, suggesting that at least part of the similar response during blood perfusion is an artifact, and therefore not representative of a physiological process. Unexpectedly, the TD during 1/2 s muscle contractions under KHBB perfusion was not different from TD values obtained during blood perfusion. The small TD could partially be explained by the intracellular stored O_2, as well as dynamic O_2 supply from the high buffer flow rate. Comparison of NIRS signals during contractions with blood perfusion versus KHBB perfusion suggested a Mb contribution of 57 ± 18 % to the NIRS signal during blood perfusion. However, these results were variable and uncertain because of possible optical pathlength changes in Hb-free versus blood perfusion.

References

1. **Bangsbo J**. Muscle oxygen uptake in humans at onset of and during intense exercise. *Acta Physiologica Scandinavica* 168: 457-464, 2000.

2. **Bangsbo J, Gibala MJ, Krustrup P, González-Alonso J, and Saltin B**. Enhanced pyruvate dehydrogenase activity does not affect muscle O2 uptake at onset of intense exercise in humans. *American Journal of Physiology-Regulatory, Integrative and Comparative Physiology* 282: R273-R280, 2002.

3. **Bangsbo J, Krustrup P, González-Alonso J, Boushel R, and Saltin B**. Muscle oxygen kinetics at onset of intense dynamic exercise in humans. *American Journal of Physiology-Regulatory, Integrative and Comparative Physiology* 279: R899-R906, 2000.

4. **Behnke BJ, Barstow TJ, Kindig CA, McDonough P, Musch TI, and Poole DC**. Dynamics of oxygen uptake following exercise onset in rat skeletal muscle. *Respiratory physiology & neurobiology* 133: 229-239, 2002.

5. **Boushel R, Langberg H, Olesen J, Gonzales‐Alonzo J, Bülow J, and Kjaer M**. Monitoring tissue oxygen availability with near infrared spectroscopy (NIRS) in health and disease. *Scandinavian Journal of Medicine & Science in Sports* 11: 213-222, 2001.

6. **Boushel R, Pott F, Madsen P, Rådegran G, Nowak M, Quistorff B, and Secher N**. Muscle metabolism from near infrared spectroscopy during rhythmic handgrip in humans. *European Journal of Applied Physiology and Occupational Physiology* 79: 41-48, 1998.

7. **Costes F, Barthelemy JC, Feasson L, Busso T, Geyssant A, and Denis C**. Comparison of muscle near-infrared spectroscopy and femoral blood gases during steady-state exercise in humans. *Journal of Applied Physiology* 80: 1345-1350, 1996.

8. **Endo M, Okada Y, Rossiter HB, Ooue A, Miura A, Koga S, and Fukuba Y**. Kinetics of pulmonary and femoral artery blood flow and their relationship during repeated bouts of heavy exercise. *European journal of applied physiology* 95: 418-430, 2005.

9. **Ferrari M, and Quaresima V**. Review: Near infrared brain and muscle oximetry: from the discovery to current applications. *Journal of Near Infrared Spectroscopy* 20: 1, 2012.

10. **González‐Alonso J, Quistorff B, Krustrup P, Bangsbo J, and Saltin B**. Heat production in human skeletal muscle at the onset of intense dynamic exercise. *The Journal of physiology* 524: 603-615, 2000.

11. **Goodwin ML, Hernandez A, Lai N, Cabrera ME, and Gladden LB**. VO_2 on-kinetics in isolated canine muscle in situ during slowed convective O_2 delivery. *Journal of Applied Physiology* 112: 9-19, 2012.

12. **Grassi B, Gladden LB, Samaja M, Stary CM, and Hogan MC**. Faster adjustment of O2delivery does not affect V˙ o 2 on-kinetics in isolated in situ canine muscle. *Journal of Applied Physiology* 85: 1394, 1998.

13. **Grassi B, Gladden LB, Samaja M, Stary CM, and Hogan MC**. Faster adjustment of O2delivery does not affect V˙ o 2 on-kinetics in isolated in situ canine muscle. *Journal of Applied Physiology* 85: 1394-1403, 1998.

14. **Grassi B, Hogan MC, Greenhaff PL, Hamann JJ, Kelley KM, Aschenbach WG, Constantin‐Teodosiu D, and Gladden LB**. Oxygen uptake on‐kinetics in dog gastrocnemius in situ following activation of pyruvate dehydrogenase by dichloroacetate. *The Journal of physiology* 538: 195-207, 2002.

15. **Grassi B, Hogan MC, Kelley KM, Aschenbach WG, Hamann JJ, Evans RK, Patillo RE, and Gladden LB**. Role of convective O2 delivery in determiningV˙ o 2 on-kinetics in canine muscle contracting at peak V˙ o 2. *Journal of Applied Physiology* 89: 1293-1301, 2000.

16. **Grassi B, Hogan MC, Kelley KM, Howlett RA, and Gladden LB**. Effects of nitric oxide synthase inhibition by l‐NAME on oxygen uptake kinetics in isolated canine muscle in situ. *The Journal of physiology* 568: 1021-1033, 2005.

17. **Henry FM**. Aerobic oxygen consumption and alactic debt in muscular work. *Journal of Applied Physiology* 3: 427-438, 1951.

18. **Hernández A, Goodwin ML, Lai N, Cabrera ME, McDonald JR, and Gladden LB**. Contraction-by-contraction V̇o2 and computer-controlled pump perfusion as novel techniques to study skeletal muscle metabolism in situ. *Journal of Applied Physiology* 108: 705-712, 2010.

19. **Hernandez A, McDonald JR, Lai N, and Gladden LB**. A prior bout of contractions speeds VO2 and blood flow on-kinetics and reduces the VO2 slow-component amplitude in canine skeletal muscle contracting in situ. *Journal of Applied Physiology* 108: 1169-1176, 2010.

20. **Hill AV, Long C, and Lupton H**. Muscular exercise, lactic acid and the supply and utilisation of oxygen. *Proceedings of the Royal Society of London Series B, Containing Papers of a Biological Character* 97: 155-176, 1924.

21. **Howlett RA, Heigenhauser GJF, and Spriet LL**. Skeletal muscle metabolism during high-intensity sprint exercise is unaffected by dichloroacetate or acetate infusion. *Journal of Applied Physiology* 87: 1747-1751, 1999.

22. **Hughson RL, Shoemaker JK, Tschakovsky ME, and Kowalchuk JM**. Dependence of muscle VO2 on blood flow dynamics at onset of forearm exercise. *Journal of Applied Physiology* 81: 1619-1626, 1996.

23. **Jones AM, and Poole DC**. *Oxygen uptake kinetics in sport, exercise and medicine*. Taylor & Francis, 2005.

24. **Jones AM, Wilkerson DP, Koppo K, Wilmshurst S, and Campbell IT**. Inhibition of nitric oxide synthase by L-NAME speeds phase II pulmonary VO2 kinetics in the transition to moderate-intensity exercise in man. *The Journal of physiology* 552: 265-272, 2003.

25. **Jones AM, Wilkerson DP, Wilmshurst S, and Campbell IT**. Influence of L-NAME on pulmonary O2 uptake kinetics during heavy-intensity cycle exercise. *Journal of Applied Physiology* 96: 1033-1038, 2004.

26. **Kim MB, Ward DS, Cartwright CR, Kolano J, Chlebowski S, and Henson LC**. Estimation of jugular venous O2 saturation from cerebral oximetry or arterial O2 saturation during isocapnic hypoxia. *Journal of Clinical Monitoring and Computing* 16: 191-199, 2000.

27. **Kindig CA, Howlett RA, Stary CM, Walsh B, and Hogan MC**. Effects of acute creatine kinase inhibition on metabolism and tension development in isolated single myocytes. *Journal of Applied Physiology* 98: 541-549, 2005.

28. **Kindig CA, Kelley KM, Howlett RA, Stary CM, and Hogan MC**. Assessment of O2 uptake dynamics in isolated single skeletal myocytes. *Journal of Applied Physiology* 94: 353-357, 2003.

29. **Kindig CA, McDonough P, Erickson HH, and Poole DC**. Effect of L-NAME on oxygen uptake kinetics during heavy-intensity exercise in the horse. *Journal of Applied Physiology* 91: 891-896, 2001.

30. **Kindig CA, McDonough P, Erickson HH, and Poole DC**. Nitric oxide synthase inhibition speeds oxygen uptake kinetics in horses during moderate domain running. *Respiratory physiology & neurobiology* 132: 169-178, 2002.

31. **Kishi K, Kawaguchi M, Yoshitani K, Nagahata T, and Furuya H**. Influence of patient variables and sensor location on regional cerebral oxygen saturation measured by INVOS 4100 near-infrared spectrophotometers. *Journal of Neurosurgical Anesthesiology* 15: 302, 2003.

32. **Krustrup P, Ferguson RA, Kjær M, and Bangsbo J**. ATP and heat production in human skeletal muscle during dynamic exercise: higher efficiency of anaerobic than aerobic ATP resynthesis. *The Journal of physiology* 549: 255-269, 2003.

33. **Lador F, Kenfack MA, Moia C, Cautero M, Morel DR, Capelli C, and Ferretti G**. Simultaneous determination of the kinetics of cardiac output, systemic O2 delivery, and lung O2 uptake at exercise onset in men. *American Journal of Physiology-Regulatory, Integrative and Comparative Physiology* 290: R1071-R1079, 2006.

34. **Lai N, Gladden LB, Carlier PG, and Cabrera ME**. Models of muscle contraction and energetics. *Drug Discovery Today: Disease Models* 5: 273-288, 2009.

35. **Mancini DM, Bolinger L, Li H, Kendrick K, Chance B, and Wilson JR**. Validation of near-infrared spectroscopy in humans. *Journal of Applied Physiology* 77: 2740-2747, 1994.

36. **Masuda K, Takakura H, Furuichi Y, Iwase S, and Jue T**. NIRS measurement of O 2 dynamics in contracting blood and buffer perfused hindlimb muscle. *Oxygen Transport to Tissue XXXI* 323-328, 2010.

37. **Maxwell L, Barclay JK, Mohrman DE, and Faulkner JA**. Physiological characteristics of skeletal muscles of dogs and cats. *American Journal of Physiology-Cell Physiology* 233: C14-C18, 1977.

38. **McCully KK, and Hamaoka T**. Near-infrared spectroscopy: what can it tell us about oxygen saturation in skeletal muscle. *Exercise & Sport Sciences Reviews* 28: 123-127, 2000.

39. **McDonald JR, Grassi B, Lai N, Hogan MC, Sun Y, and Gladden LB**. Effect of Hypoxia with Matched Convective O2 Delivery on VO2 On-Kinetics in Canine Skeletal Muscle in situ. *Medicine & Science in Sports & Exercise* 42: 42, 2010.

40. **Owen-Reece H, Smith M, Elwell C, and Goldstone J**. Near infrared spectroscopy. *British Journal of Anaesthesia* 82: 418-426, 1999.

41. **Parolin ML, Spriet LL, Hultman E, Matsos MP, Hollidge-Horvat MG, Jones NL, and Heigenhauser GJF**. Effects of PDH activation by dichloroacetate in human skeletal muscle during exercise in hypoxia. *American Journal of Physiology-Endocrinology And Metabolism* 279: E752-E761, 2000.

42. **Roman BB, Meyer RA, and Wiseman RW**. Phosphocreatine kinetics at the onset of contractions in skeletal muscle of MM creatine kinase knockout mice. *American Journal of Physiology-Cell Physiology* 283: C1776-C1783, 2002.

43. **Rossiter H, Ward S, Doyle V, Howe F, Griffiths J, and Whipp B**. Inferences from pulmonary O2 uptake with respect to intramuscular [phosphocreatine] kinetics during moderate exercise in humans. *The Journal of physiology* 518: 921-932, 1999.

44. **Rossiter HB, Ward SA, Howe FA, Wood DM, Kowalchuk JM, Griffiths JR, and Whipp BJ**. Effects of dichloroacetate on VO2 and intramuscular 31P metabolite kinetics during high-intensity exercise in humans. *Journal of Applied Physiology* 95: 1105-1115, 2003.

45. **Seiyama A, Hazeki O, and Tamura M**. Noninvasive quantitative analysis of blood oxygenation in rat skeletal muscle. *Journal of Biochemistry* 103: 419-424, 1988.

46. **Stainsby WN, and Welch HG**. Lactate metabolism of contracting dog skeletal muscle in situ. *American Journal of Physiology--Legacy Content* 211: 177-183, 1966.

47. **Takakura H, Masuda K, Hashimoto T, Iwase S, and Jue T**. Quantification of myoglobin deoxygenation and intracellular partial pressure of O2 during muscle contraction during haemoglobin‐free medium perfusion. *Experimental physiology* 95: 630-640, 2010.

48. **Tran TK, Sailasuta N, Kreutzer U, Hurd R, Chung Y, Mole P, Kuno S, and Jue T**. Comparative analysis of NMR and NIRS measurements of intracellular in human skeletal muscle. *American Journal of Physiology-Regulatory, Integrative and Comparative Physiology* 276: R1682-R1690, 1999.

49. **Tschakovsky M, and Hughson R**. Interaction of factors determining oxygen uptake at the onset of exercise. *Journal of Applied Physiology* 86: 1101-1113, 1999.

50. **Whipp BJ, Seard C, and Wasserman K**. Oxygen deficit-oxygen debt relationships and efficiency of anaerobic work. *Journal of Applied Physiology* 28: 452-456, 1970.

51. **Wilson JR, Mancini D, McCully K, Ferraro N, Lanoce V, and Chance B**. Noninvasive detection of skeletal muscle underperfusion with near-infrared spectroscopy in patients with heart failure. *Circulation* 80: 1668-1674, 1989.

52. **Wüst RCI, Grassi B, Hogan MC, Howlett RA, Gladden LB, and Rossiter HB**. Kinetic control of oxygen consumption during contractions in self‐perfused skeletal muscle. *The Journal of physiology* 589: 3995-4009, 2011.

53. **Wüst RCI, McDonald JR, Ferguson BS, Sun Y, Rogatzki MJ, Spires J, Kowalchuk JM, Gladden LB, and Rossiter HB**. Slowed muscle VO2 kinetics with raised metabolism: not dependent on blood flow or recruitment dynamics. *Poster at ACSM annual meeting* 2012.

54. **Yoshitani K, Kawaguchi M, Iwata M, Sasaoka N, Inoue S, Kurumatani N, and Furuya H**. Comparison of changes in jugular venous bulb oxygen saturation and cerebral oxygen saturation during variations of haemoglobin concentration under propofol and sevoflurane anaesthesia. *British Journal of Anaesthesia* 94: 341-346, 2005.

CUMULATIVE REFERENCES

1. **Adcock LM, Wafelman LS, Hegemier S, Moise AA, Speer ME, Contant CF, and Goddard-Finegold J**. Neonatal intensive care applications of near-infrared spectroscopy. *Clinics in Perinatology* 26: 893, 1999.

2. **Arena R, Myers J, Aslam SS, Varughese EB, and Peberdy MA**. Peak VO2 and VE/VCO2 slope in patients with heart failure: a prognostic comparison. *American Heart Journal* 147: 354-360, 2004.

3. **Arena R, and Sietsema KE**. Cardiopulmonary exercise testing in the clinical evaluation of patients with heart and lung disease. *Circulation* 123: 668-680, 2011.

4. **Artinis**. Optical Imaging Made Easy, User Manual Oxymon Mk III. edited by BV AMS2006.

5. **Babcock MA, Paterson DH, Cunningham DA, and Dickinson JR**. Exercise on-transient gas exchange kinetics are slowed as a function of age. *Medicine & Science in Sports & Exercise* 26: 440, 1994.

6. **Bangsbo J**. Muscle oxygen uptake in humans at onset of and during intense exercise. *Acta Physiologica Scandinavica* 168: 457-464, 2000.

7. **Bangsbo J, Gibala MJ, Krustrup P, González-Alonso J, and Saltin B**. Enhanced pyruvate dehydrogenase activity does not affect muscle O2 uptake at onset of intense exercise in humans. *American Journal of Physiology-Regulatory, Integrative and Comparative Physiology* 282: R273-R280, 2002.

8. **Bangsbo J, Krustrup P, González-Alonso J, Boushel R, and Saltin B**. Muscle oxygen kinetics at onset of intense dynamic exercise in humans. *American Journal of Physiology-Regulatory, Integrative and Comparative Physiology* 279: R899-R906, 2000.

9. **Behnke BJ, Barstow TJ, Kindig CA, McDonough P, Musch TI, and Poole DC**. Dynamics of oxygen uptake following exercise onset in rat skeletal muscle. *Respiratory physiology & neurobiology* 133: 229-239, 2002.

10. **Boushel R, Langberg H, Olesen J, Gonzales‐Alonzo J, Bülow J, and Kjaer M**. Monitoring tissue oxygen availability with near infrared spectroscopy (NIRS) in health and disease. *Scandinavian Journal of Medicine & Science in Sports* 11: 213-222, 2001.

11. **Boushel R, Pott F, Madsen P, Rådegran G, Nowak M, Quistorff B, and Secher N**. Muscle metabolism from near infrared spectroscopy during rhythmic handgrip in humans. *European Journal of Applied Physiology and Occupational Physiology* 79: 41-48, 1998.

12. **Brandenburg SL, Reusch J, Bauer TA, Jeffers BW, Hiatt WR, and Regensteiner JG**. Effects of exercise training on oxygen uptake kinetic responses in women with type 2 diabetes. *Diabetes Care* 22: 1640-1646, 1999.

13. **Brass EP, and Hiatt WR**. Acquired skeletal muscle metabolic myopathy in atherosclerotic peripheral arterial disease. *Vascular Medicine* 5: 55-59, 2000.

14. **Burnley M, Jones AM, Carter H, and Doust JH**. Effects of prior heavy exercise on phase II pulmonary oxygen uptake kinetics during heavy exercise. *Journal of Applied Physiology* 89: 1387-1396, 2000.

15. **Campbell MK, and Farrell SO**. *Biochemistry Fourth Edition*. 2003, p. 104-113.

16. **Chung Y, Molé PA, Sailasuta N, Tran TK, Hurd R, and Jue T**. Control of respiration and bioenergetics during muscle contraction. *American Journal of Physiology-Cell Physiology* 288: C730-C738, 2005.

17. **Costes F, Barthelemy JC, Feasson L, Busso T, Geyssant A, and Denis C**. Comparison of muscle near-infrared spectroscopy and femoral blood gases during steady-state exercise in humans. *Journal of Applied Physiology* 80: 1345-1350, 1996.

18. **DeLorey DS, Kowalchuk JM, and Paterson DH**. Relationship between pulmonary O2 uptake kinetics and muscle deoxygenation during moderate-intensity exercise. *Journal of Applied Physiology* 95: 113, 2003.

19. **Endo M, Okada Y, Rossiter HB, Ooue A, Miura A, Koga S, and Fukuba Y**. Kinetics of pulmonary and femoral artery blood flow and their relationship during repeated bouts of heavy exercise. *European journal of applied physiology* 95: 418-430, 2005.

20. **Endo MY, Kobayakawa M, Kinugasa R, Kuno S, Akima H, Rossiter HB, Miura A, and Fukuba Y**. Thigh muscle activation distribution and pulmonary VO2 kinetics during

moderate, heavy, and very heavy intensity cycling exercise in humans. *American Journal of Physiology-Regulatory, Integrative and Comparative Physiology* 293: R812-R820, 2007.

21. **Ferrari M, and Quaresima V**. Review: Near infrared brain and muscle oximetry: from the discovery to current applications. *Journal of Near Infrared Spectroscopy* 20: 1, 2012.

22. **Ferreira LF, Koga S, and Barstow TJ**. Dynamics of noninvasively estimated microvascular O2 extraction during ramp exercise. *Journal of Applied Physiology* 103: 1999-2004, 2007.

23. **Giannini I, Ferrari M, Carpi A, and Fasella P**. Rat brain monitoring by near-infrared spectroscopy: an assessment of possible clinical significance. *Physiological Chemistry and Physics* 14: 295, 1982.

24. **Gladden LB**. Lactate metabolism: a new paradigm for the third millennium. *The Journal of physiology* 558: 5-30, 2004.

25. **González - Alonso J, Quistorff B, Krustrup P, Bangsbo J, and Saltin B**. Heat production in human skeletal muscle at the onset of intense dynamic exercise. *The Journal of physiology* 524: 603-615, 2000.

26. **Goodwin ML, Hernandez A, Lai N, Cabrera ME, and Gladden LB**. VO_2 on-kinetics in isolated canine muscle in situ during slowed convective O_2 delivery. *Journal of Applied Physiology* 112: 9-19, 2012.

27. **Grassi B, Gladden LB, Samaja M, Stary CM, and Hogan MC**. Faster adjustment of O2delivery does not affect V˙ o 2 on-kinetics in isolated in situ canine muscle. *Journal of Applied Physiology* 85: 1394-1403, 1998.

28. **Grassi B, Gladden LB, Samaja M, Stary CM, and Hogan MC**. Faster adjustment of O2delivery does not affect V˙ o 2 on-kinetics in isolated in situ canine muscle. *Journal of Applied Physiology* 85: 1394, 1998.

29. **Grassi B, Gladden LB, Stary CM, Wagner PD, and Hogan MC**. Peripheral O2 diffusion does not affect V˙ o 2 on-kinetics in isolated in situ canine muscle. *Journal of Applied Physiology* 85: 1404-1412, 1998.

30. **Grassi B, Hogan MC, Greenhaff PL, Hamann JJ, Kelley KM, Aschenbach WG, Constantin‐Teodosiu D, and Gladden LB**. Oxygen uptake on‐kinetics in dog gastrocnemius in situ following activation of pyruvate dehydrogenase by dichloroacetate. *The Journal of physiology* 538: 195-207, 2002.

31. **Grassi B, Hogan MC, Kelley KM, Aschenbach WG, Hamann JJ, Evans RK, Patillo RE, and Gladden LB**. Role of convective O2 delivery in determining$\dot{V}$o 2 on-kinetics in canine muscle contracting at peak $\dot{V}$o 2. *Journal of Applied Physiology* 89: 1293-1301, 2000.

32. **Grassi B, Hogan MC, Kelley KM, Howlett RA, and Gladden LB**. Effects of nitric oxide synthase inhibition by l‐NAME on oxygen uptake kinetics in isolated canine muscle in situ. *The Journal of physiology* 568: 1021-1033, 2005.

33. **Grassi B, Marzorati M, Lanfranconi F, Ferri A, Longaretti M, Stucchi A, Vago P, Marconi C, and Morandi L**. Impaired oxygen extraction in metabolic myopathies: Detection and quantification by near‐infrared spectroscopy. *Muscle & Nerve* 35: 510-520, 2007.

34. **Grassi B, Morandi L, Pogliaghi S, Rampichini S, Marconi C, and Cerretelli P**. Functional evaluation of patients with metabolic myopathies during exercise. *Medicine & Science in Sports & Exercise* 34: S78, 2002.

35. **Grassi B, Pogliaghi S, Rampichini S, Quaresima V, Ferrari M, Marconi C, and Cerretelli P**. Muscle oxygenation and pulmonary gas exchange kinetics during cycling exercise on-transitions in humans. *Journal of Applied Physiology* 95: 149-158, 2003.

36. **Grassi B, Poole DC, Richardson RS, Knight DR, Erickson BK, and Wagner PD**. Muscle O2 uptake kinetics in humans: implications for metabolic control. *Journal of Applied Physiology* 80: 988-998, 1996.

37. **Grassi B, Rossiter HB, Hogan MC, Howlett RA, Harris JE, Goodwin ML, Dobson JL, and Gladden LB**. Faster O uptake kinetics in canine skeletal muscle in situ after acute creatine kinase inhibition. *The Journal of physiology* 589: 221-233, 2011.

38. **Henry FM**. Aerobic oxygen consumption and alactic debt in muscular work. *Journal of Applied Physiology* 3: 427-438, 1951.

39. **Henson LC, Calalang C, Temp JA, and Ward DS**. Accuracy of a cerebral oximeter in healthy volunteers under conditions of isocapnic hypoxia. *Anesthesiology* 88: 58, 1998.

40. **Hernández A, Goodwin ML, Lai N, Cabrera ME, McDonald JR, and Gladden LB**. Contraction-by-contraction V̇o2 and computer-controlled pump perfusion as novel techniques to study skeletal muscle metabolism in situ. *Journal of Applied Physiology* 108: 705-712, 2010.

41. **Hernandez A, McDonald JR, Lai N, and Gladden LB**. A prior bout of contractions speeds VO2 and blood flow on-kinetics and reduces the VO2 slow-component amplitude in canine skeletal muscle contracting in situ. *Journal of Applied Physiology* 108: 1169-1176, 2010.

42. **Hiatt WR, Wolfel EE, Meier RH, and Regensteiner JG**. Superiority of treadmill walking exercise versus strength training for patients with peripheral arterial disease. Implications for the mechanism of the training response. *Circulation* 90: 1866-1874, 1994.

43. **Hill AV, Long C, and Lupton H**. Muscular exercise, lactic acid and the supply and utilisation of oxygen. *Proceedings of the Royal Society of London Series B, Containing Papers of a Biological Character* 97: 155-176, 1924.

44. **Hochachka P, and Matheson G**. Regulating ATP turnover rates over broad dynamic work ranges in skeletal muscles. *Journal of Applied Physiology* 73: 1697-1703, 1992.

45. **Hogan MC, Bebout DE, Wagner PD, and West JB**. Maximal O2 uptake of in situ dog muscle during acute hypoxemia with constant perfusion. *Journal of Applied Physiology* 69: 570-576, 1990.

46. **Houston ME**. *Biochemistry primer for exercise science*. Human Kinetics Publishers, 2006.

47. **Howlett RA, Heigenhauser GJF, and Spriet LL**. Skeletal muscle metabolism during high-intensity sprint exercise is unaffected by dichloroacetate or acetate infusion. *Journal of Applied Physiology* 87: 1747-1751, 1999.

48. **Hughson RL, and Kowalchuk JM**. Kinetics of oxygen uptake for submaximal exercise in hyperoxia, normoxia, and hypoxia. *Canadian Journal of Applied Physiology* 20: 198-210, 1995.

49. **Hughson RL, Shoemaker JK, Tschakovsky ME, and Kowalchuk JM**. Dependence of muscle VO2 on blood flow dynamics at onset of forearm exercise. *Journal of Applied Physiology* 81: 1619-1626, 1996.

50. **Jones AM, and Poole DC**. *Oxygen uptake kinetics in sport, exercise and medicine*. Taylor & Francis, 2005.

51. **Jones AM, Wilkerson DP, Koppo K, Wilmshurst S, and Campbell IT**. Inhibition of nitric oxide synthase by L-NAME speeds phase II pulmonary VO2 kinetics in the transition to moderate-intensity exercise in man. *The Journal of physiology* 552: 265-272, 2003.

52. **Jones AM, Wilkerson DP, Wilmshurst S, and Campbell IT**. Influence of L-NAME on pulmonary O2 uptake kinetics during heavy-intensity cycle exercise. *Journal of Applied Physiology* 96: 1033-1038, 2004.

53. **Katz A, and Sahlin K**. Effect of decreased oxygen availability on NADH and lactate contents in human skeletal muscle during exercise. *Acta Physiologica Scandinavica* 131: 119-127, 1987.

54. **Kim MB, Ward DS, Cartwright CR, Kolano J, Chlebowski S, and Henson LC**. Estimation of jugular venous O2 saturation from cerebral oximetry or arterial O2 saturation during isocapnic hypoxia. *Journal of Clinical Monitoring and Computing* 16: 191-199, 2000.

55. **Kindig CA, Howlett RA, Stary CM, Walsh B, and Hogan MC**. Effects of acute creatine kinase inhibition on metabolism and tension development in isolated single myocytes. *Journal of Applied Physiology* 98: 541-549, 2005.

56. **Kindig CA, Kelley KM, Howlett RA, Stary CM, and Hogan MC**. Assessment of O2 uptake dynamics in isolated single skeletal myocytes. *Journal of Applied Physiology* 94: 353-357, 2003.

57. **Kindig CA, McDonough P, Erickson HH, and Poole DC**. Effect of L-NAME on oxygen uptake kinetics during heavy-intensity exercise in the horse. *Journal of Applied Physiology* 91: 891-896, 2001.

58. **Kindig CA, McDonough P, Erickson HH, and Poole DC**. Nitric oxide synthase inhibition speeds oxygen uptake kinetics in horses during moderate domain running. *Respiratory physiology & neurobiology* 132: 169-178, 2002.

59. **Kishi K, Kawaguchi M, Yoshitani K, Nagahata T, and Furuya H**. Influence of patient variables and sensor location on regional cerebral oxygen saturation measured by INVOS 4100 near-infrared spectrophotometers. *Journal of Neurosurgical Anesthesiology* 15: 302, 2003.

60. **Krogh A, and Lindhard J**. The regulation of respiration and circulation during the initial stages of muscular work. *The Journal of physiology* 47: 112-136, 1913.

61. **Krustrup P, Ferguson RA, Kjær M, and Bangsbo J**. ATP and heat production in human skeletal muscle during dynamic exercise: higher efficiency of anaerobic than aerobic ATP resynthesis. *The Journal of physiology* 549: 255-269, 2003.

62. **Lador F, Kenfack MA, Moia C, Cautero M, Morel DR, Capelli C, and Ferretti G**. Simultaneous determination of the kinetics of cardiac output, systemic O2 delivery, and lung O2 uptake at exercise onset in men. *American Journal of Physiology-Regulatory, Integrative and Comparative Physiology* 290: R1071-R1079, 2006.

63. **Lai N, Gladden LB, Carlier PG, and Cabrera ME**. Models of muscle contraction and energetics. *Drug Discovery Today: Disease Models* 5: 273-288, 2009.

64. **Lai N, Zhou H, Saidel GM, Wolf M, McCully K, Gladden LB, and Cabrera ME**. Modeling oxygenation in venous blood and skeletal muscle in response to exercise using near-infrared spectroscopy. *Journal of Applied Physiology* 106: 1858-1874, 2009.

65. **Lovell AT, Owen-Reece H, Elwell CE, Smith M, and Goldstone JC**. Continuous measurement of cerebral oxygenation by near infrared spectroscopy during induction of anesthesia. *Anesthesia & Analgesia* 88: 554-554, 1999.

66. **Mancini DM, Bolinger L, Li H, Kendrick K, Chance B, and Wilson JR**. Validation of near-infrared spectroscopy in humans. *Journal of Applied Physiology* 77: 2740-2747, 1994.

67. **Masuda K, Takakura H, Furuichi Y, Iwase S, and Jue T**. NIRS measurement of O 2 dynamics in contracting blood and buffer perfused hindlimb muscle. *Oxygen Transport to Tissue XXXI* 323-328, 2010.

68. **Maxwell L, Barclay JK, Mohrman DE, and Faulkner JA**. Physiological characteristics of skeletal muscles of dogs and cats. *American Journal of Physiology-Cell Physiology* 233: C14-C18, 1977.

69. **McCully KK, and Hamaoka T**. Near-infrared spectroscopy: what can it tell us about oxygen saturation in skeletal muscle. *Exercise & Sport Sciences Reviews* 28: 123-127, 2000.

70. **McDonald JR, Grassi B, Lai N, Hogan MC, Sun Y, and Gladden LB**. Effect of Hypoxia with Matched Convective O2 Delivery on VO2 On-Kinetics in Canine Skeletal Muscle in situ. *Medicine & Science in Sports & Exercise* 42: 42, 2010.

71. **Mehagnoul‐Schipper DJ, van der Kallen BFW, Colier WNJM, van der Sluijs MC, van Erning LJTO, Thijssen HOM, Oeseburg B, Hoefnagels WHL, and Jansen RWMM**. Simultaneous measurements of cerebral oxygenation changes during brain activation by near‐infrared spectroscopy and functional magnetic resonance imaging in healthy young and elderly subjects. *Human Brain Mapping* 16: 14-23, 2002.

72. **Moyle J**. *Pulse oximetry*. Blackwell Pub., 2002.

73. **Munro MJ, Walker AM, and Barfield CP**. Hypotensive extremely low birth weight infants have reduced cerebral blood flow. *Pediatrics* 114: 1591-1596, 2004.

74. **Ordway GA, and Garry DJ**. Myoglobin: an essential hemoprotein in striated muscle. *Journal of Experimental Biology* 207: 3441, 2004.

75. **Owen-Reece H, Smith M, Elwell C, and Goldstone J**. Near infrared spectroscopy. *British Journal of Anaesthesia* 82: 418-426, 1999.

76. **Page AJ, Coyle S, Keane TM, Naughton TJ, Markham C, and Ward T**. Distributed monte carlo simulation of light transportation in tissue. In: *Parallel and Distributed Processing Symposium, 2006 IPDPS 2006 20th International*2006, p. 4 pp.

77. **Palange P, Galassetti P, Mannix E, Farber M, Manfredi F, Serra P, and Carlone S**. Oxygen effect on O2 deficit and VO2 kinetics during exercise in obstructive pulmonary disease. *Journal of Applied Physiology* 78: 2228-2234, 1995.

78. **Parolin ML, Spriet LL, Hultman E, Hollidge-Horvat MG, Jones NL, and Heigenhauser GJF**. Regulation of glycogen phosphorylase and PDH during exercise in human skeletal muscle during hypoxia. *American Journal of Physiology-Endocrinology And Metabolism* 278: E522-E534, 2000.

79. **Parolin ML, Spriet LL, Hultman E, Matsos MP, Hollidge-Horvat MG, Jones NL, and Heigenhauser GJF**. Effects of PDH activation by dichloroacetate in human skeletal muscle during exercise in hypoxia. *American Journal of Physiology-Endocrinology And Metabolism* 279: E752-E761, 2000.

80. **Poole DC, Barstow TJ, McDonough P, and Jones AM**. Control of oxygen uptake during exercise. *Medicine & Science in Sports & Exercise* 40: 462, 2008.

81. **Poortmans JR**. *Principles of Exercise Biochemistry (Medicine and Sport Science)*. S Karger Pub, 2003.

82. **Powers SK, and Howley ET**. *Exercise Physiology : Theory and Application to Fitness and Performance - 6th edition*. McGraw-Hill, 2006.

83. **Richardson R, Noyszewski E, Kendrick K, Leigh J, and Wagner P**. Myoglobin O2 desaturation during exercise. Evidence of limited O2 transport. *Journal of Clinical Investigation* 96: 1916, 1995.

84. **Richardson RS, Leek BT, Gavin TP, Haseler LJ, Mudaliar SRD, Henry R, Mathieu-Costello O, and Wagner PD**. Reduced mechanical efficiency in chronic obstructive pulmonary disease but normal peak VO2 with small muscle mass exercise. *American Journal of Respiratory and Critical Care Medicine* 169: 89-96, 2004.

85. **Richardson RS TK, Haseler LJ, Jordan M, Wagner PD**. Increased VO2max with right-shifted Hb-O2 dissociation curve at a constant O2 delivery in dog muscle in situ. *Journal of Applied Physiology* 84: 995-1002, 1998.

86. **Roman BB, Meyer RA, and Wiseman RW**. Phosphocreatine kinetics at the onset of contractions in skeletal muscle of MM creatine kinase knockout mice. *American Journal of Physiology-Cell Physiology* 283: C1776-C1783, 2002.

87. **Rossiter H, Ward S, Doyle V, Howe F, Griffiths J, and Whipp B**. Inferences from pulmonary O2 uptake with respect to intramuscular [phosphocreatine] kinetics during moderate exercise in humans. *The Journal of physiology* 518: 921-932, 1999.

88. **Rossiter H, Ward S, Doyle V, Howe F, Griffiths J, and Whipp B**. Inferences from pulmonary O2 uptake with respect to intramuscular [phosphocreatine] kinetics during moderate exercise in humans. *The Journal of physiology* 518: 921-932, 1999.

89. **Rossiter HB**. Exercise: kinetic considerations for gas exchange. *Comprehensive Physiology* 2011.

90. **Rossiter HB, Ward SA, Howe FA, Wood DM, Kowalchuk JM, Griffiths JR, and Whipp BJ**. Effects of dichloroacetate on VO2 and intramuscular 31P metabolite kinetics during high-intensity exercise in humans. *Journal of Applied Physiology* 95: 1105-1115, 2003.

91. **Sahlin K, Tonkonogi M, and Söderlund K**. Energy supply and muscle fatigue in humans. *Acta Physiologica Scandinavica* 162: 261-266, 1998.

92. **Sako T, Hamaoka T, Higuchi H, Kurosawa Y, and Katsumura T**. Validity of NIR spectroscopy for quantitatively measuring muscle oxidative metabolic rate in exercise. *Journal of Applied Physiology* 90: 338-344, 2001.

93. **Schenkman KA, Marble DR, Burns DH, and Feigl EO**. Myoglobin oxygen dissociation by multiwavelength spectroscopy. *Journal of Applied Physiology* 82: 86, 1997.

94. **Seiyama A, Hazeki O, and Tamura M**. Noninvasive quantitative analysis of blood oxygenation in rat skeletal muscle. *Journal of Biochemistry* 103: 419-424, 1988.

95. **Sietsema KE, Cooper D, Perloff JK, Rosove M, Child J, Canobbio M, Whipp B, and Wasserman K**. Dynamics of oxygen uptake during exercise in adults with cyanotic congenital heart disease. *Circulation* 73: 1137, 1986.

96. **Stainsby WN, and Welch HG**. Lactate metabolism of contracting dog skeletal muscle in situ. *American Journal of Physiology--Legacy Content* 211: 177-183, 1966.

97. **Stamler JS, and Meissner G**. Physiology of nitric oxide in skeletal muscle. *Physiological Reviews* 81: 209-237, 2001.

98. **Takakura H, Masuda K, Hashimoto T, Iwase S, and Jue T**. Quantification of myoglobin deoxygenation and intracellular partial pressure of O2 during muscle contraction during haemoglobin‐free medium perfusion. *Experimental physiology* 95: 630-640, 2010.

99. **Towse TF, Slade JM, Ambrose JA, DeLano MC, and Meyer RA**. Quantitative analysis of the postcontractile blood-oxygenation-level-dependent (BOLD) effect in skeletal muscle. *Journal of Applied Physiology* 111: 27, 2011.

100. **Tran TK, Sailasuta N, Kreutzer U, Hurd R, Chung Y, Mole P, Kuno S, and Jue T**. Comparative analysis of NMR and NIRS measurements of intracellular in human skeletal muscle. *American Journal of Physiology-Regulatory, Integrative and Comparative Physiology* 276: R1682-R1690, 1999.

101. **Tschakovsky M, and Hughson R**. Interaction of factors determining oxygen uptake at the onset of exercise. *Journal of Applied Physiology* 86: 1101-1113, 1999.

102. **Van der Zee P, Arridge S, Cope M, and Delpy D**. The effect of optode positioning on optical pathlength in near infrared spectroscopy of brain. *Advances in Experimental Medicine and Biology* 277: 79-84, 1990.

103. **Whipp BJ, Seard C, and Wasserman K**. Oxygen deficit-oxygen debt relationships and efficiency of anaerobic work. *Journal of Applied Physiology* 28: 452-456, 1970.

104. **Whipp BJ, Ward SA, Lamarra N, Davis JA, and Wasserman K**. Parameters of ventilatory and gas exchange dynamics during exercise. *Journal of Applied Physiology* 52: 1506-1513, 1982.

105. **Wilson JR, Mancini D, McCully K, Ferraro N, Lanoce V, and Chance B**. Noninvasive detection of skeletal muscle underperfusion with near-infrared spectroscopy in patients with heart failure. *Circulation* 80: 1668-1674, 1989.

106. **Wüst RCI, Grassi B, Hogan MC, Howlett RA, Gladden LB, and Rossiter HB**. Kinetic control of oxygen consumption during contractions in self‐perfused skeletal muscle. *The Journal of physiology* 589: 3995-4009, 2011.

107. **Wüst RCI, McDonald JR, Ferguson BS, Sun Y, Rogatzki MJ, Spires J, Kowalchuk JM, Gladden LB, and Rossiter HB**. Is there a time-delay in muscle oxygen uptake at the onset of contractions? *Poster at The Biomedical Basis of Elite Performance* 2012.

108. **Wüst RCI, McDonald JR, Ferguson BS, Sun Y, Rogatzki MJ, Spires J, Kowalchuk JM, Gladden LB, and Rossiter HB**. Slowed muscle VO2 kinetics with raised metabolism: not dependent on blood flow or recruitment dynamics. *Poster at ACSM annual meeting* 2012.

109. **Wyatt J, Cope M, Delpy D, Richardson C, Edwards A, Wray S, and Reynolds E**. Quantitation of cerebral blood volume in human infants by near-infrared spectroscopy. *Journal of Applied Physiology* 68: 1086-1091, 1990.

110. **Wyatt JS**. Noninvasive assessment of cerebral oxidative metabolism in the human newborn. *Journal of the Royal College of Physicians of London* 28: 126, 1994.

111. **Yoshitani K, Kawaguchi M, Iwata M, Sasaoka N, Inoue S, Kurumatani N, and Furuya H**. Comparison of changes in jugular venous bulb oxygen saturation and cerebral

oxygen saturation during variations of haemoglobin concentration under propofol and sevoflurane anaesthesia. *British Journal of Anaesthesia* 94: 341-346, 2005.

112. **Zoladz JA, Gladden LB, Hogan MC, Nieckarz Z, and Grassi B**. Progressive recruitment of muscle fibers is not necessary for the slow component of VO2 kinetics. *Journal of Applied Physiology* 105: 575-580, 2008.